REGIONE DEL VENETO
ULSS2 MARCA TREVIGIANA

INFORMAZIONI PERSONALI

Cognome e nome	**TALIN ANNA**
Anno di nascita	1993
U.O.C. di appartenenza	Medicina Nucleare
Incarico attuale	Dirigente medico
Telefono ufficio	0422 322300
E-mail istituzionale	anna.talin@aulss2.veneto.it

ESPERIENZA LAVORATIVA

• Date (da – a)	**26/01/2021 – 03/02/2025**
• Nome e indirizzo del datore di lavoro	Università degli studi di Brescia, Piazza del Mercato, 15, 25121 Brescia BS
• Tipo di azienda o settore	Scuola di Specializzazione in Medicina Nucleare
• Tipo di impiego	Medico Specializzando in Medicina Nucleare
• Principali mansioni e responsabilità	Diagnostica e terapia medico-nucleare

• Date (da – a)	**01/11/2021 – 28/02/2022**
• Nome e indirizzo del datore di lavoro	ATS Brescia, Viale Duca degli Abruzzi, 15 – 25124 Brescia BS
• Tipo di azienda o settore	Pubblica Amministrazione
• Tipo di impiego	Medico di Continuità Assistenziale
• Principali mansioni e responsabilità	Guardia medica – visite

• Date (da – a)	**01/06/2021 – 31/01/2022**
• Nome e indirizzo del datore di lavoro	ASST Spedali Civili di Brescia, Piazzale Spedali Civili, 1, 25123 Brescia BS
• Tipo di azienda o settore	Pubblica Amministrazione
• Tipo di impiego	Dirigente Medico
• Principali mansioni e responsabilità	Medico Vaccinatore per emergenza COVID-19

• Date (da – a)	**01/11/2020 – 23/01/2021**
• Nome e indirizzo del datore di lavoro	ULSS7 PEDEMONTANA, Via Boldrini, 1, 36016 Thiene VI
• Tipo di azienda o settore	Pubblica Amministrazione
• Tipo di impiego	Medico di Unità Speciale di Continuità Assistenziale (U.S.C.A)
• Principali mansioni e responsabilità	Visite domiciliari per emergenza COVID 19

• Date (da – a)	**28/12/2020 – 08/01/2021**
• Nome e indirizzo del datore di lavoro	Dott.ssa Ida Busin MMG, Viale Europa 13, 36030 San Vito di Leguzzano (VI)
• Tipo di azienda o settore	Medico di medicina generale

• Tipo di impiego	Medico sostituto
• Principali mansioni e responsabilità	Sostituzione medico di medicina generale

• Date (da – a)	**06/10/2020 – 22/10/2020**
• Nome e indirizzo del datore di lavoro	Dott.ssa Elena Martinello MMG, Via F.lli Bandiera 111, 36034 Malo (VI)
• Tipo di azienda o settore	Medico di medicina generale
• Tipo di impiego	Medico sostituto
• Principali mansioni e responsabilità	Sostituzione medico di medicina generale

• Date (da – a)	**09/10/2020 – 09/10/2020**
• Nome e indirizzo del datore di lavoro	Dott.ssa Giulia Sartori MMG, Via Milano 25, 36030 Monte di Malo (VI)
• Tipo di azienda o settore	Medico di medicina generale
• Tipo di impiego	Medico sostituto
• Principali mansioni e responsabilità	Sostituzione medico di medicina generale

• Date (da – a)	**31/08/2020 – 16/9/2020**
• Nome e indirizzo del datore di lavoro	Dott.ssa Ida Busin MMG, Viale Europa 13, 36030 San Vito di Leguzzano (VI),
• Tipo di azienda o settore	Medico di medicina generale
• Tipo di impiego	Medico sostituto
• Principali mansioni e responsabilità	Sostituzione medico di medicina generale

ISTRUZIONE E FORMAZIONE

• Date (da – a)	**26/01/2021 – 03/02/2025**
• Nome e tipo di istituto di istruzione o formazione	Università degli Studi di Brescia, Piazza del Mercato, 15, 25121 Brescia BS
• Principali materie / abilità professionali oggetto dello studio	Medicina Nucleare
• Qualifica conseguita	Diploma di specializzazione in medicina nucleare
• Livello nella classificazione nazionale (se pertinente)	Specializzazione post-laurea (livello 8 EQF)

• Data	**30/06/2020**
• Nome e tipo di istituto	Ordine provinciale dei Medici Chirurghi e Odontoiatri di Vicenza
• Qualifica conseguita	Iscrizione all'albo
• Numero di iscrizione	06744

• Date (da – a)	**25/06/2020**
• Nome e tipo di istituto di istruzione o formazione	Università degli studi di Padova, Via VIII Febbraio, 2, 35122 Padova PD
• Principali materie / abilità professionali oggetto dello studio	Medicina e Chirurgia
• Qualifica conseguita	Abilitazione alla professione di Medico Chirurgo
• Livello nella classificazione nazionale (se pertinente)	

• Date (da – a)	**Ottobre 2012 – 25/06/2020**
• Nome e tipo di istituto di istruzione o formazione	Università degli studi di Padova, Via VIII Febbraio, 2, 35122 Padova PD
• Principali materie / abilità professionali oggetto dello studio	Medicina e chirurgia
• Qualifica conseguita	Laurea magistrale in medicina e chirurgia (LM41)
• Livello nella classificazione nazionale (se pertinente)	Laurea magistrale (livello 7 EQF)

• Date (da – a)	**Ottobre 2007 – Luglio 2012**
• Nome e tipo di istituto di istruzione o formazione	Liceo Scientifico Statale "Giovanni Battista Quadri", Viale Giosuè Carducci, 17, 36100 Vicenza VI
• Principali materie / abilità professionali oggetto dello studio	Indirizzo Scientifico Tecnologico
• Qualifica conseguita	Diploma di maturità scientifica
• Livello nella classificazione nazionale (se pertinente)	Istruzione secondaria superiore (livello 4 EQF)

CAPACITÀ E COMPETENZE PERSONALI

Acquisite nel corso della vita e della carriera ma non necessariamente riconosciute da certificati e diplomi ufficiali.

Capacità di lavorare in armonia con team multidisciplinari e di favorire un ambiente di lavoro positivo, empatia e comunicazione efficace con i pazienti, gestione dello stress, problem solving, adattabilità ai cambiamenti, dedizione alla formazione e all'aggiornamento scientifico.

MADRELINGUA **ITALIANO**

ALTRE LINGUE

INGLESE

• Capacità di lettura	ECCELLENTE
• Capacità di scrittura	BUONA
• Capacità di espressione orale	BUONA

COMPETENZE INFORMATICHE

Esperienza nell'uso di: pacchetti microsoft office (Word, Excel, Power point), software per la refertazione e la gestione dei pazienti (Fenix), software per imaging medico (Xeleris per l'elaborazione e l'analisi delle immagini di medicina nucleare), piattaforme di archiviazione degli esami diagnostici (PACS), programmi per analisi statistiche in ambito medico (MedCalc), navigazione web e ricerca scientifica mediante banche dati (PubMed, Scopus, Cochrane Library), strumenti per l'organizzazione delle fonti e la creazione automatica di bibliografie (Mendeley).

ULTERIORI INFORMAZIONI

Partecipazione come autrice ad articoli scientifici pubblicati, e come uditrice a congressi europei di Medicina Nucleare (vedi allegati).

ALLEGATI

ALLEGATO 1, ALLEGATO 2, ALLEGATO 3, ALLEGATO 4, ALLEGATO 5. ALLEGATO 6

DATA 13/03/2025

FIRMATO

Annals of Nuclear Medicine
https://doi.org/10.1007/s12149-025-02026-7

ORIGINAL ARTICLE

The prognostic role of staging [18F]PSMA-1007 PET/CT volumetric and dissemination features in prostate cancer

Domenico Albano[1,2] · Alessandro Temponi[3] · Francesco Bertagna[1,2] · Nazareno Suardi[4] · Anna Talin[2] · Marco Lorenzo Bonù[5] · Luca Triggiani[5]

Received: 15 January 2025 / Accepted: 5 February 2025
© The Author(s) 2025

Abstract

Background This study aimed the role of volumetric and dissemination features of staging [18F]PSMA-1007 PET/CT in predicting progression-free survival (PFS) in patients with prostate cancer (PCa) and their relationship with the main clinical data (ISUP grade groups, number of lesions, PSA).

Methods We included 164 patients with high-risk PCa who underwent baseline [18F]PSMA-1007 PET/CT. With the help of LIFEx version 7.7, the main volumetric and dissemination PET parameters were semi-automatically extracted: PSMA-prostate tumor volume (PSMA-TV), PSMA-prostate total lesion (PSMA-TL), PSMA total TV (PSMA-TTV), PSMA total TL (PSMA-TTL) and Dmax corrected for body-surface-area ($Dmax_{bsa}$). Spearman rank correlations between semiquantitative PET features and the clinical variables were analyzed. PFS estimates were plotted with the Kaplan–Meier method.

Results A high correlation was seen between the number of lesions and both PSMA-TTL (r 0.725), and Dmaxbsa (r 0.935). A moderate correlation was registered between PSA and PSMA-TTV (r 0.333), PSMA-TTL (r 0.441), $Dmax_{bsa}$ (r 0.333), as well as between number of lesions and PSMA-TTV (r 0.342).

After a median follow-up of 17 months (range 2–45), relapse/progression happened in 17 patients (10%). PSA level, presence of distant metastases at staging, PSMA-TV, PSMA-TL, PSMA-TTL and $Dmax_{bsa}$ were significantly associated with PFS at univariate analysis, but only the presence of distant metastases, PSMA-TTL and $Dmax_{bsa}$ were confirmed to be independent prognostic factors.

Conclusion Volumetric and dissemination features derived by staging [18F]PSMA-1007 PET/CT were significantly correlated with PSA and number of lesions. The combination of PSMA-TTL and $Dmax_{bsa}$ was the best predictor of PFS and may help to better stratify PCa patients.

Keywords Prostate cancer · PET/CT · Dmax · PSMA · Nuclear medicine

Introduction

Prostate-specific membrane antigen (PSMA) positron emission tomography/computed tomography (PET/CT) is a non-invasive diagnostic tool with superior accuracy over conventional imaging in studying prostate cancer (PCa) [1]. PSMA PET/CT is an examination exploiting the higher expression of PSMA by PCa cells compared to healthy prostatic tissue. Such exams have already been widely explored for staging purposes [2], both for recurrent [3] and newly diagnosed diseases. After a substantial body of evidence was accumulated regarding [68 Ga]Ga-PSMA imaging, recent advances in logistics and the enhanced availability of [18F]PSMA-1007 have significantly broadened their use in PSMA PET imaging for PCa. Indeed, [18F]PSMA-1007 shows the best

✉ Domenico Albano
doalba87@libero.it

1 Nuclear Medicine, University of Brescia, Brescia, Italy

2 Nuclear Medicine Department, ASST Spedali Civili di Brescia, Brescia, Italy

3 Clinical Engineering, ASST Spedali Civili of Brescia, Brescia, Italy

4 Department of Urology, University of Brescia, Brescia, Italy

5 Radiation Oncology, ASST Spedali Civili di Brescia, Brescia, Italy

Published online: 17 February 2025

diagnostic performances in the study of local disease, due to the prevalent non-urinary excretion, but incidental non-neoplastic bone uptakes reported in the literature, called unspecific bone uptake (UBU), are quite frequent and their meaning not yet clear [4, 5].

Beyond qualitative analysis [1], (semi)quantitative parameters derived from PET images are emerging as potentially useful in stratifying better PCa patients. Among them, standardized uptake value (SUV) is the parameter more commonly used due to its velocity and ease of extraction [6], but also more influenced by external factors, as confirmed by decades of studies with fluorodeoxyglucose (FDG) PET/CT. For these reasons, other quantitative features expressing tumor burden have been studied, like PSMA tumor volume (PSMA-TV) and PSMA total lesion (PSMA-TL). The prognostic role of these parameters was explored in several researches, especially in metastatic castration-resistant prostate cancer (mCRPC) receiving [177Lu]PSMA-617 therapy [7–9], second-line chemotherapy with cabazitaxel [10] and taxane-based chemotherapy (docetaxel) [11, 12]. In these analyses, high PSMA uptake seems to be associated with worse outcomes. So far, less data and heterogeneous are available for locally confined disease and primary staging of PCa [13, 14]. Recently, a new FDG PET-derived parameter was introduced for studying hematological malignancies and predicting their survival: the maximum tumor dissemination (Dmax) [15]. Dmax is a simple three-dimensional variable that represents the maximal distance between the two farthest PET lesions with increased uptake. Moreover, only preliminary and scarce findings are available about the potential role of Dmax in PCa [16, 17].

Therefore, this retrospective study aimed to investigate the usefulness of volumetric and dissemination [18F]PSMA-1007 PET/CT features measured at staging in predicting the outcome in PCa. Second aim was to investigate the correlation between different quantitative PSMA parameters, with the main clinical factors (such as Gleason grade, number of lesions, PSA values).

Materials and methods

Patients

This study was a monocentric retrospective study that analyzed all patients who underwent [18F]PSMA-1007 PET/CT between January 2021 and January 2024. Inclusion criteria were: (1) histologically confirmed PCa; (2) availability of staging [18F]PSMA-1007 PET/CT; (3) at least 12 months as follow–up; (4) not having received any treatment for prostate cancer before PET/CT (not androgen deprivation therapy, chemotherapy or radiotherapy). Instead, the exclusion criteria were: (1) a history of treatment for prostate cancer; (2) PSMA not avid primary prostatic tumor; (3) metastatic castration-resistant prostate cancer (mCRPC) patients. Finally, 164 patients were recruited in this study. For each patient, the main clinical and epidemiological data were collected, such as age, PSA value at diagnosis, ISUP grade group (1–3 considered as early, 4–5 as advanced), ECOG performance status, lactate dehydrogenase (LDH) level, alkaline phosphatase (ALP) level, international society of urological pathology (ISUP) grading and clinical stage. The study adhered to the Declaration of Helsinki and was approved by the local ethics committee. Written informed consent was provided by the recruited patients. The patients were treated according to the institutional protocols at the time of the diagnosis, following the main international guidelines.

[18F]PSMA-1007 PET/CT imaging and interpretation

[18F]PSMA-1007 PET/CT scans were acquired about 90 min (range, 80–110 min) after the administration of a median dose of 305 MBq (279–340 MBq) of [18F]PSMA-1007, according to the current guidelines [1]. All PET/CT studies were performed using dedicated state-of-the-art tomographs Discovery ST and 690 (GE Healthcare). CT images acquisition parameters: 120 kV, 30–400 mA, and 0.984:1/39.37 pitch.

All PET/CT scans were revised for a visual and semiquantitative point of view by an experienced nuclear medicine physician with more than 10 years of experience (DA). who was blinded to the patient's outcome. For visual analysis, every area of increased focal uptake higher than the background was reported as suspected of malignancy. Images were evaluated for the detection of the primary tumor, locoregional and extra-pelvic lymph nodes, bone and visceral metastases. For semiquantitative analysis, the feature extraction was performed using LIFEx version 7.7 [18]. By using the MTV protocol in this software, areas with PSMA uptake SUVmax $\geq$ 2.0 were segmented automatically in the whole body obtaining volumes of interest (VOI). Later, all VOIs were visually checked to confirm their pathological meaning or to remove in case of sites of physiologic (such as kidneys, bladder, intestine…) or benign uptakes according to PSMA-rads criteria [19]. To exclude UBU, a frequent unspecific finding with [18F]PSMA-1007, we applied the BUMP score as suggested in the literature [4]. The SUVmax threshold of 41% was applied to all remaining VOIs thought to be related to prostate cancer. Subsequently, we derived the PSMA-prostate tumor volume (PSMA-TV) as the volume measured in the primary prostatic lesion or lesions in case of multifocality of disease, PSMA-prostate total lesion (PSMA-TL) determined as PSMA-TV x SUVmean, the PSMA total tumor volume (PSMA-TTV) as the sum of all PSMA-TV values of the tumor-associated VOIs (prostatic lesion, metastatic lymph nodes and distant metastases), and

PSMA total TL (PSMA-TTL) value was determined as the sum of all PSMA-TL values. Subsequently for the calculation of Dmax, LIFEx software applying the Euclidean formula measured the distance between all pairs of lesions (including all lesions) recording the greatest lesion distance. Subsequently, Dmax was normalized by the patient body surface area ($_{bsa}$) calculated according to the Du Bois method to get Dmaxbsa. In the case of PET/CT with only prostate lesion, Dmax was defined as 0. For the calculation of Dmax, UBUs were excluded.

Statistical analysis

MedCalc version 18 for Windows (Ostend, Belgium) was the software that we used for our statistical analyses. The categorical variables were described as simple and relative frequencies, while the numeric variables were described as average, median, standard deviations (SD) and range. To evaluate the correlation between volumetric/dissemination PET features and the main clinical-epidemiological variables (PSA, number of lesions, Gleason grade) we utilized Spearman's rank correlation coefficient. A p value of 0.05 was considered statistically significant.

Receiver operating characteristic (ROC) curve was plotted to estimate the optimal thresholds values of PSMA-TV, PSMA-TL, PSMA-TTV, PSMA-TTL, $DMAX_{bsa}$ for predicting PFS. PFS was estimated with the Kaplan–Meier method and log-rank test. PFS was defined as the interval from the date of diagnosis until recurrence or progression (considered as biochemical if PSA value increased again after treatment and/or structural defined as enlargement of original lesion or appearance of new lesions at imaging studies). Univariate and multivariate analyses were carried out using the Cox proportional hazard model to evaluate factors that predict PFS. Confidence interval (CI) was selected as 95% and a two-sided p value of less than 0.05 was accepted as significant.

To avoid multicollinearity impact between PET metrics, PSMA-TV and PSMA-TL were considered separately in the multivariate analysis. The same behavior for PSMA-TVV and PSMA-TTL.

Results

Population features and PET/CT findings

A total of 164 males (average age 70.4 years) were enrolled. The main patient's characteristics are outlined in Table 1. The mean PSA level was 31.6 ng/ml ranging from 1.63 to 490 ng/ml, the mean ALP level was 74 U/L ranging from 39 to 102 U/L, and the mean LDH level was 186 U/L ranging from 125 to 225 U/L. Most patients had advanced ISUP grade ($n = 108$) and ECOG performance status was 0 in 80% of cases. [18F]PSMA-1007 PET/CT revealed no evidence of metastases in 111 patients (67%), whereas the remaining 53 (33%) patients had PSMA-avid metastases. Among them, 48 had skeletal metastases and 5 had abdominal lymph nodal metastases. UBUs were registered in 36 cases (22%) and in 27 patients were the only bone uptake reported in the scan.

Table 1 Baseline features of our population (164 patients)

	Patients n (%)	Average ± SD	Median (range)
Age		70.4 ± 7.8	72 (48–87)
ISUP grade			
1–3	56 (34%)		
4–5	108 (66%)		
ECOG performance status			
0	131 (80%)		
1–2	33 (20%)		
M status at staging			
M0	116 (81%)		
M1	48 (29%)		
D'amico risk classification			
Low-intermediate	19 (12%)		
High	145 (88%)		
PSA level (ng/mL)		31.6 ± 52.7	13(1.63–490)
ALP level (U/L)		74 ± 29.3	77.5 (39–102)
LDH level (U/L)		186 ± 43.6	185 (125–225)
PSMA-TV (cm^3)		8.2 ± 7.8	5 (1.5–46)
PSMA-TTV (cm^3)		87.9 ± 119	49.5 (3.5–880)
PSMA-TL		35.9 ± 75.7	9.95 (1.5–511)
PSMA-TTL		232.7 ± 404	90 (5–2560)
$Dmax_{bsa}$ (cm)		7.7 ± 10.2	4.6 (0–41.5)
Therapies after PET/CT			
Local			
Surgery	44 (27%)		
Radiotherapy	40 (24%)		
Radiotherapy + ADT	32 (20%)		
Systemic			
ADT	19 (12%)		
ADT + ARPI	20 (12%)		
ADT + Chemotherapy	9 (5%)		
Follow-up (months)		16 ± 9.5	14 (2–45)

ADT androgen deprivation therapy, *ARPI* androgen receptor signaling inhibitor, *LDH* lactate dehydrogenase, *ALP* alkaline phosphatase, *ISUP* international society of urological pathology, *PSA* prostate specific antigen, *ECOG* Eastern cooperative oncology group, *PSMA-TV* PSMA-prostate tumor volume, *TL* prostate total lesion, *TTV* total tumor volume, *TTL* total TL

After PET/CT, patients received local or systemic treatment according to the clinical features and stage: 44 underwent prostatectomy, 72 radiotherapy (with ADT in 32 cases, without ADT in 40), 19 only ADT, 20 ADT + androgen receptor signaling inhibitor and 9 to ADT plus chemotherapy. The median PSMA-TV was 5 cm^3 (range 1.5–46 cm^3), median PSMA-TL 9.95 (1.5–511), median PSMA-TTV 49.5 cm^3 (3.5–880 cm^3), median PSMA-TTL 90 (5–2560) and median $Dmax_{bsa}$ 4.6 (0–41.5).

Correlation between PET-quantitative parameters and clinical features

Among the quantitative PSMA PET parameters investigated, several (PSMA-TTV, PSMA-TTL and Dmaxbsa) were significantly associated with PSA value and number of lesions (Fig. 1) (all p value < 0.001). A strong correlation was present among number of lesions and PSMA-TTL (Spearman rho 0.725), and among the number of lesions and $Dmax_{bsa}$ (Spearman rho 0.935); instead a moderate correlation was registered between PSA and PSMA-TTV (Spearman rho 0.333), PSA and PSMA-TTL (Spearman rho 0.441), PSA and $Dmax_{bsa}$ (Spearman rho 0.333), number of lesions and PSMA-TTV (Spearman rho 0.342). Instead other PET features, such as PSMA-TV and PSMA-TL, were not associated with the clinical variables evaluated ($p > 0.05$). The same for the association between all PET parameters and GG ($p > 0.05$).

Prognostic role of [18F]PSMA-1007 PET/CT in predicting progression-free survival

For the prognostic evaluation of the role of volumetric and dissemination features, we dichotomized these variables applying ROC curve analysis. The best threshold derived was represented in Table 2. At a median follow-up of 17 months (range 2–45), relapse or progression of disease occurred in 17 patients (10%) with a median time of 10 months (range: 2–25 months) from the staging [18F] PSMA-1007 PET/CT. One-year and 3-year PFS were 93% and 90%, respectively. At univariate analysis, PSA level, presence of distant metastases at staging, PSMA-TV, PSMA-TL, PSMA-TTL and $Dmax_{bsa}$ were significantly correlated with the risk of progression/relapse (Table 3, Fig. 2). The other clinical features and PSMA-TTV were not associated with PFS. At the multivariate test, only distant metastases, PSMA-TTL and $Dmax_{bsa}$ were confirmed to be independent prognostic factors concerning PFS. We combined PSMA-TTL and $Dmax_{bsa}$ to derive three groups: (1) with low PSMA-TTL(≤ 140) and low $Dmax_{bsa}$(≤ 15.66); (2) low PSMA-TTL(≤ 140) + high $Dmax_{bsa}$ (> 15.66) or high PSMA-TTL(> 140) + low $Dmax_{bsa}$ (≤ 15.66); (3) high PSMA-TTL(> 140) and low $Dmax_{bsa}$ (> 15.66). This score stratified better patients PFS as shown in Fig. 3. Patients with high PSMA-TTL and high $Dmax_{bsa}$ had lower PFS compared to the other two groups. The median PFS of patients with high PSMA-TTL and high $Dmax_{bsa}$ was 10.3 months, of the patients

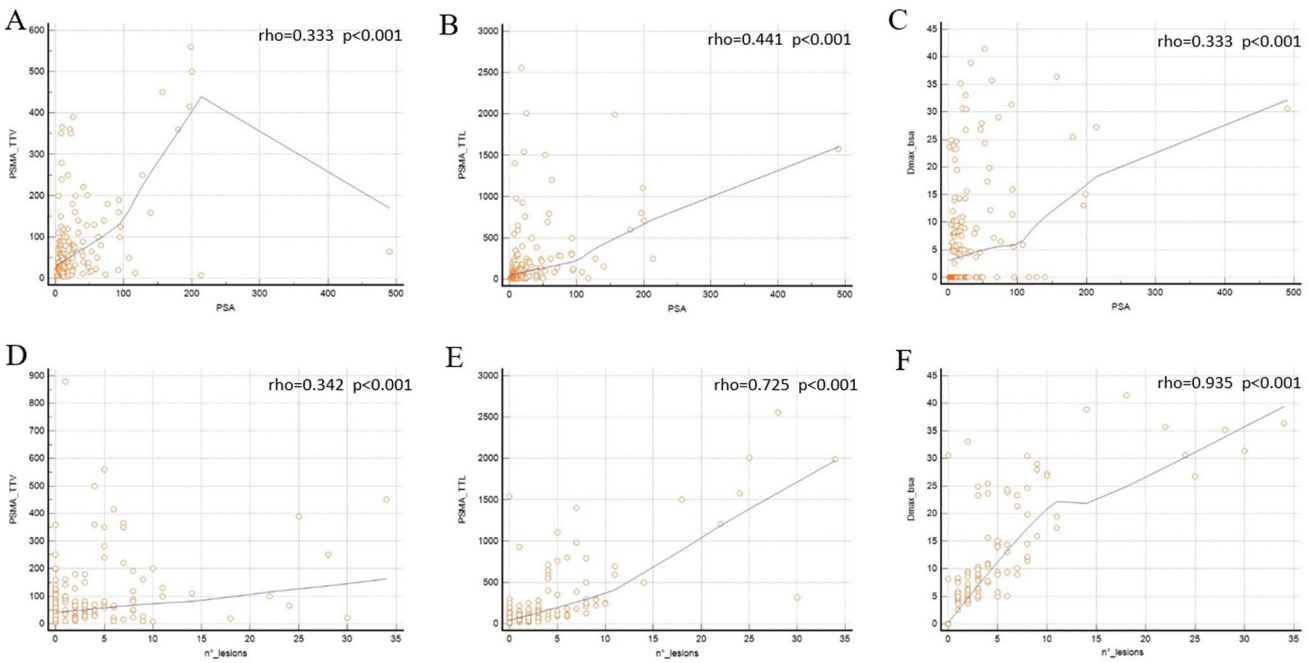

Fig. 1 Correlation between PSA and PSMA-TTV (**A**), PSMA-TTL (**B**) and Dmax (**C**). Correlation between number of lesions (n°) and PSMA-TTV (**D**), PSMA-TTL (**E**) and Dmax (**F**)

Table 2 semiquantitative PET/CT parameters cutoff calculated using receiver operating characteristic (ROC) curve analysis considering the entire population

	ROC curve for PFS				
Parameter	cutoff	AUC (95% CI)	*p* value	Sens (95% CI)	Spec (95% CI)
PSMA-TV cm^3	13.3	0.697 (0.620–0.766)	0.004	52.9% (27.8–77)	83% (75.9–88.7)
PSMA-TTV cm^3	78	0.632 (0.554–0.706)	0.074	52.9% (27.8–77)	70.7% (62.7–78)
PSMA-TL	50	0.841 (0.775–0.893)	< 0.001	64.7% (38.3–85.8)	89.1% (82.9–93.6)
PSMA-TTL	140	0.819 (0.752–0.875)	< 0.001	82.4% (56.6–96.2)	70.1% (62–77.3)
$Dmax_{bsa}$ cm	15.66	0.856 (0.793–0.906)	< 0.001	70.6% (44–89.7)	89.1% (82.9–93.6)

PFS progression free survival, *AUC* area under curve, *CI* confidence interval, *sens:* sensibility *spec:* specificity

Table 3 univariate and multivariate analyses for PFS

	Univariate analysis		Multivariate analysis	
	p value	HR (95% CI)	*p* value	HR (95% CI)
Age	0.180	1.201 (0.900–2.528)		
ECOG performance status	0.445	1.989 (0.728–2.888)		
ISUP	0.949	1.038 (0.382–2.787)		
PSA	0.018	3.459 (1.331–8.989)	0.125	1.528 (0.898–3.669)
LDH	0.568	1.989 (0.700–3.958)		
ALP	0.547	2.582 (0.600–4.564)		
D'amico risk group high	0.663	1.265 (0.438–3.653)		
M + at staging	< 0.001	7.854 (2.828–21.816)	0.021	3.982 (1.229–12.901)
PSMA-TV cm^3*	0.002	5.729 (1.833–17.907)	0.250	2.546 (0.890–4.001)
PSMA-TTV cm^3*	0.107	2.281 (0.836–6.227)		
PSMA-TL*	< 0.001	54.519 (14.216–209.085)	0.066	3.102 (0.929–10.374)
PSMA-TTL*	< 0.001	7.269 (2.702–19.532)	0.022	1.580(1.268–1.892)
$Dmax_{bsa}$ cm *	< 0.001	51.148 (14.919–184.340)	0.001	2.078 (1.023–3.136)

PFS progression-free survival, *HR* hazard ratio, *CI* confidence interval

*Variables dichotomized using cutoff values after ROC analysis reported in Table 2

PSMa-TV and PSMA-TL; PSMA-TTV and PSMA-TLL were evaluated separately due to the collinearity relationship

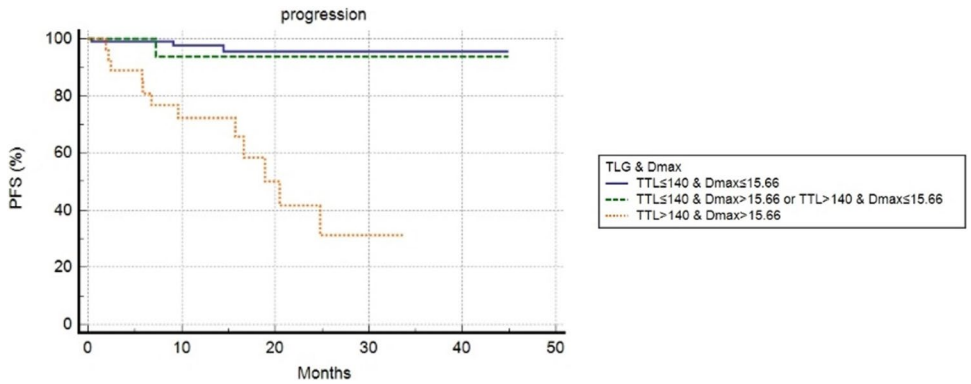

Fig. 2 Progression-free survival curves according to PSMA-TV (**A**), PSMA-TL (**B**), PSMA-TTV (**C**), PSMA-TTL (**D**), $Dmax_{bsa}$ (**E**)

with low PSMA-TTL + high $Dmax_{bsa}$ or high PSMA-TTL + low $Dmax_{bsa}$ was 15.2 months, of patients with low PSMA-TTL and low $Dmax_{bsa}$ 16.5 months.

Discussion

The research of early and accurate not-invasive biomarkers to predict treatment response and/or survival are desirable with the aim to maximize treatment efficacy and improve

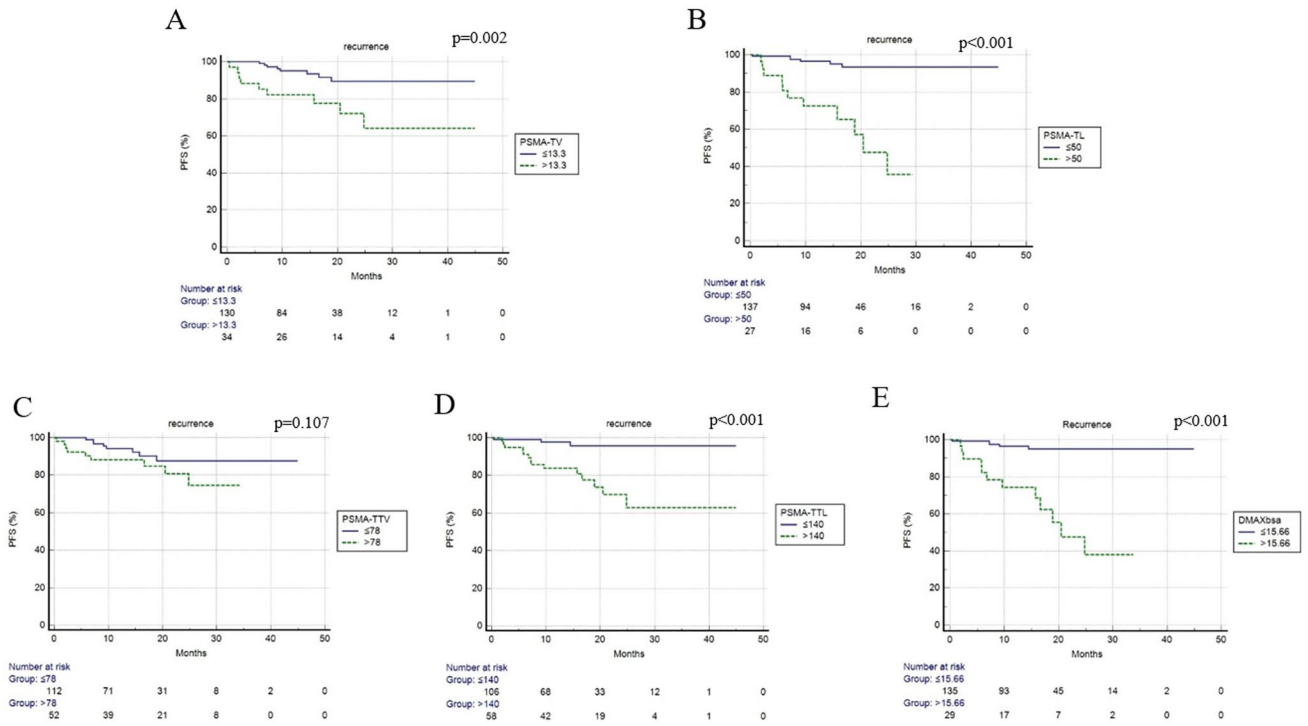

Fig. 3 Progression-free survival curves according to the combination of PSMA-TTL and $Dmax_{bsa}$. Blue line represents patients with low PSMA-TTL and low $Dmax_{bsa}$; green line patients with low PSMA-TTL and high $Dmax_{bsa}$ or high PSMA-TTL and low $Dmax_{bsa}$; yellow line patients with high PSMA-TTL and high $Dmax_{bsa}$

outcome. For PCa patients, PSMA PET/CT had been emerged as a fundamental imaging tool in the staging of high-risk patients, due to the ability to detect distant disease better than conventional imaging including CT and bone scan. Besides visual analysis, several (semi)quantitative parameters derived by PET images are available in the literature. The impact of tumor FDG PET volumetric features on the prognosis of several oncological diseases, especially lymphoma, had been already described [20–22]. These parameters, known as MTV and TLG, reflect at the same time tumor morphological and functional activity of the disease. The same rationale may be applied also in the PCa setting, of course with PSMA-radiopharmaceuticals. First, Schmuck et al. investigated the role of volumetric PSMA variables (PSMA-TV and PSMA-TL) in treatment response evaluation demonstrating a useful yield of these volumetric markers in predicting therapy failure and a linear correlation between these PET features and PSA value [23]. Similar findings were subsequently confirmed by other studies in patients with biochemical recurrence or bone metastases from PCa [24, 25]. But in these cases, only TV and TL were evaluated and not biomarkers expressing global diffuse disease such as PSMA-TTV, PSMA-TTL or Dmax. Instead, PSMA-derived volumetric features calculated at staging PSMA PET/CT were measured and tested only in a few studies [12, 13], showing in all a positive association between PSA and PET features (Table 4). Particularly, PSMA-TTV and PSMA-TTL were demonstrated to be the factors with the highest correlations with PSA. This association is logical because PSA is a protein expressed by cancer cells, thus can be indirectly considered as the expression of tumor burden disease with exceptions in cases of disease not producing PSA. Sometimes also association with age and GG was reported but not confirmed in all papers. This evidence is in agreement with our analysis, where PSMA-TTV and PSMA-TTL were showed to be moderately correlated with PSA and number of the lesions, while no significant correlations with GG were derived.

The prognostic impact of baseline PET volumetric variables in not mCRPC patients in terms of PFS was studied only in one study [13]. In this retrospective work, Zou et al. recruited 59 newly diagnosed PCa and examined the prognostic role of several PSMA PET features (SUVmax, SUVpeak, SUVmean, PSMA-TV, PSMA-TL, PSMA-TTV, PSMA-TTL) showing that only PSMA-TTL was an independent prognostic factor together with GG.

However, volumetric features did not include in their definition the pattern of distribution of disease and the number of lesions PSMA-positive. High-risk PCa patients may have extraprostatic disease and plural distant localizations. On the other hand, Dmax is a feature that

Table 4 the summary of the main studies about the role of semiquantitative PSMA parameters measured at baseline PET/CT

First author	Year	Number of patients	Radiotracer	Main results
Aksu A	2021	88	^{68} Ga-PSMA	PSMA-TTV and PSMA-TTL correlated with PSA. PSMA-TV and PSMA-TL correlated with extension of disease, GG and risk-group
Santos A	2021	46	^{68} Ga-PSMA	PSMA-TTV and PSMA-TTL not correlated with PSA, age, GG
Zschaeck S	2022	135*	^{68} Ga-PSMA	PSMA-TV moderately correlated with PSA and GG
Zou Q	2020	59	^{68} Ga-PSMA	PSMA-TTV and PSMA-TTL correlated with PSA and GG PSMA-TTL independently correlated with PFS
Telli TA	2022	54**	^{68} Ga-PSMA	PSMA-TTV and PSMA-TTL correlated with PSA PSMA-TTV independently correlated with OS

GG gleason grade, *PSMA-TV* PSMA prostate tumor volume, *PSMA-TL* PSMA prostate total lesion, *PSMA-TTV* PSMA whole body total volume, *PSMA-TTL* PSMA whole-body total lesion

*not metastatic patients

**mCRPC patients

symbolizes the distribution and dissemination of disease with increased uptake. The possible advantages of Dmax compared to tumor burden variables are the simpleness, speed of extraction (now automated) and clinical meaning expression of patient-based spatial migration of disease [15]. Furthermore, this parameter is less influenced by technical characteristics such as kind of scanners or acquisition-reconstruction protocols. In this study, we decided to evaluate Dmax normalized by BSA to take into account the size and height of each patient. This normalization was suggested previously by other colleagues in not PCa [20, 21], but it is not yet universally shared. Previous articles [20, 21] that investigated Dmax role in PCa patients considered it as an absolute value without body correction. In the first study [16], Dmax was shown to be strongly correlated with PSA values (rho = 0.793, $p < 0.001$), PSMA-TV (rho = 0.797, $p < 0.001$) and PSMA-TTL (rho = 0.763, $p < 0.001$) and was also influenced by Gleason score grade. Instead, in another research [17] the potential prognostic role of Dmax was tested and compared with PSMA-TV and PSMA-TL demonstrating to be the only independent prognostic factor at multivariate analysis in predicting biochemical recurrence. This finding was concordant with our analysis where we revealed $Dmax_{bsa}$ as a strong predictor of PFS and moderately correlated with PSA value. In our opinion, considering Dmax without normalization for body composition is potentially a limitation because not really representative of disease distribution that is for definition affected by anthropometric characteristics. Particularly, we believe that body composition can affect the effective measurement of Dmax with a potential impact on the extraction of specific thresholds. In our analysis, the combination of PSMA-TTL and $Dmax_{bsa}$ showed to be the better combination to predict survival. Patients with both elevated PSMA-TTL and $Dmax_{bsa}$ demonstrated worse survival than others as shown in Fig. 3. This combination could perhaps be helpful to predict prognosis after first-line treatment identifying patients with a higher risk of relapse/recurrence. In the clinical scenario, this model might anticipate the imaging follow-up or associate a more aggressive therapeutic plan. Of course, this score needs to be validated in a more solid population, in more events and with a longer follow-up period.

A difference of our research between previous is the evaluation of [18F]PSMA-1007 than [Ga68]Ga-PSMA PET/CT, the radiotracer used in all studies that previously investigated semiquantitative parameters. [18F]PSMA-1007 and [Ga68]Ga-PSMA had different radiotracer biodistribution: [Ga68]Ga-PSMA PET/CT is characterized by a high urinary clearance that potentially reduces the accuracy in the evaluation of primary/local disease due to the vicinity to radioactive urine. This issue may affect the calculation of TV and TL, which now is automatic but deserves a strong manual check to be sure to avoid to surround not malignant tissues. Of course, the add of a manual modification is for definition operator-dependent and may increase the risk of error. On the other hand, [18F]PSMA-1007 had a hepatic elimination causing a higher easiness to evaluate prostatic disease and pelvic nodes and consequentially to extract TV and TL. However, one of the main limitations of [18F]PSMA-1007 is the risk to have incidental bone uptakes without radiological equivalent, called UBU [5]. To overcome this limit, we applied the BUMP score that showed a good diagnostic performance to distinguish between malignant and non-malignant bone uptake in large populations [4]. However, from a diagnostic point of view different PSMA-tracers do not seem to have statistically different performances in recurrent prostate cancer [26]. However, it is not clear if the calculation of volumetric and dissemination PET features may be significantly affected by the kind of radiotracer.

Larger studies are needed to find the best combination of prognostic variables and the factors most readily used in clinical practice for PCa.

Our research presents several limitations: first, the retrospective nature of the investigation with its known limitations. Second, the relatively short follow-up time due to the recent diffusion in the clinical practice of PSMA PET/CT in our country. Third, the lack of prostatectomy as a procedure in all patients causing the presence of GG derived by biopsy results. Despite this, so far, the present study represents the largest series of PCa patients investigated with volumetric and dissemination parameters derived from staging [18F] PSMA-1007 PET/ CT and their prognostic role.

Conclusions

In conclusion, in this study we demonstrated that volumetric and dissemination features derived by [18F]PSMA-1007 PET/CT are significantly correlated with clinical features (PSA and number of lesions) and represent useful predictors of PFS.

Funding Open access funding provided by Università degli Studi di Brescia within the CRUI-CARE Agreement.

Declarations

Conflict of interest The authors declare they have no conflict of interest.

Ethical approval All procedures performed in studies involving human participants were in accordance with the ethical standards of the institutional and/or national research committee and with the 1964 Helsinki Declaration and its later amendments or comparable ethical standards.

Informed consent Informed consent was obtained from all individual participants included in the study.

Open Access This article is licensed under a Creative Commons Attribution 4.0 International License, which permits use, sharing, adaptation, distribution and reproduction in any medium or format, as long as you give appropriate credit to the original author(s) and the source, provide a link to the Creative Commons licence, and indicate if changes were made. The images or other third party material in this article are included in the article's Creative Commons licence, unless indicated otherwise in a credit line to the material. If material is not included in the article's Creative Commons licence and your intended use is not permitted by statutory regulation or exceeds the permitted use, you will need to obtain permission directly from the copyright holder. To view a copy of this licence, visit http://creativecommons.org/licenses/by/4.0/.

References

1. Ceci F, Oprea-Lager DE, Emmett L, Adam JA, Bomanji J, Czernin J, et al. E-PSMA: the EANM standardized reporting guidelines v1.0 for PSMA-PET. Eur J Nucl Med Mol Imaging. 2021;48(5):1626–38. https://doi.org/10.1007/s00259-021-05245-y.
2. Jochumsen MR, Bouchelouche K. PSMA PET/CT for primary staging of prostate cancer: an updated overview. Semin Nucl Med. 2024;54(1):39–45. https://doi.org/10.1053/j.semnuclmed.2023.07.001.
3. Bianchi L, Castellucci P, Farolfi A, Droghetti M, Artigas C, Leite J, et al. Multicenter external validation of a nomogram for predicting positive prostate-specific membrane antigen/positron emission tomography scan in patients with prostate cancer recurrence. Eur Urol Oncol. 2023;6(1):41–8. https://doi.org/10.1016/j.euo.2021.12.002.
4. Bauckneht M, D'Amico F, Albano D, Balma M, Cabrini C, Dondi F, et al. Composite prediction score to interpret bone focal uptake in hormone-sensitive prostate cancer patients imaged with [18F] PSMA-1007 PET/CT. J Nucl Med. 2024;65(10):1577–83. https://doi.org/10.2967/jnumed.124.267751.
5. Rizzo A, Morbelli S, Albano D, Fornarini G, Cioffi M, Laudicella R, et al. The Homunculus of unspecific bone uptakes associated with PSMA-targeted tracers: a systematic review-based definition. Eur J Nucl Med Mol Imaging. 2024;51(12):3753–64. https://doi.org/10.1007/s00259-024-06797-5.
6. Chen R, Ng YL, Yang X, Zhu Y, Li L, Zhao H, et al. Comparison of parametric imaging and SUV imaging with [68 Ga]Ga-PSMA-11 using dynamic total-body PET/CT in prostate cancer. Eur J Nucl Med Mol Imaging. 2024;51(2):568–80. https://doi.org/10.1007/s00259-023-06456-1.
7. Gafita A, Bieth M, Krönke M, Tetteh G, Navarro F, Wang H, et al. qPSMA: semiautomatic software for whole-body tumor burden assessment in prostate cancer using 68Ga- PSMA11 PET/CT. J Nucl Med. 2019;60:1277–83.
8. Ferdinandus J, Violet J, Sandhu S, Hicks R, Kumar AS, Iravani A, et al. Prognostic biomarkers in men with metastatic castration-resistant prostate cancer receiving [177Lu]-PSMA-617. Eur J Nucl Med Mol Imaging. 2020;47:2322–7.
9. Seifert R, Herrmann K, Kleesiek J, Schafers M, Shah V, Xu Z, et al. Semiautomatically quantified tumor volume using (68) Ga-PSMA-11 PET as a biomarker for survival in patients with advanced prostate cancer. J Nucl Med. 2020;61:1786–92.
10. Shagera QA, Karfis I, Sideris S, Guiot T, Woff E, Martinez-Chanza N, et al. Tumor volume on PSMA PET as a prognostic biomarker in prostate cancer patients treated with cabazitaxel. Clin Nucl Med. 2023;48(9):775–80. https://doi.org/10.1097/RLU.0000000000004763.
11. Shagera QA, Artigas C, Karfis I, Critchi G, Chanza NM, Sideris S, et al. 68Ga-PSMA PET/CT for response assessment and outcome prediction in metastatic prostate cancer patients treated with taxane-based chemotherapy. J Nucl Med. 2022;63(8):1191–8. https://doi.org/10.2967/jnumed.121.263006.
12. Telli TA, Ozguven S, Alan O, Filizoglu N, Ozturk MA, Sariyar N, et al. Role of baseline 68Ga-PSMA PET/CT-derived whole-body volumetric parameters in predicting survival outcomes of metastatic castration-resistant prostate cancer patients receiving first-line treatment. Ann Nucl Med. 2022;36(11):964–75. https://doi.org/10.1007/s12149-022-01785-x.
13. Zou Q, Jiao J, Zou MH, Li MZ, Yang T, et al. Semi-automatic evaluation of baseline whole-body tumor burden as an imaging biomarker of 68Ga-PSMA-11 PET/CT in newly diagnosed prostate cancer. Abdom Radiol (NY). 2020;45(12):4202–13. https://doi.org/10.1007/s00261-020-02745-7.
14. Aksu A, Karahan Şen NP, Tuna EB, Aslan G, Çapa KG. Evaluation of 68Ga-PSMA PET/CT with volumetric parameters for staging of prostate cancer patients. Nucl Med Commun. 2021;42(5):503–9. https://doi.org/10.1097/MNM.0000000000001370.

15. Albano D, Treglia G, Dondi F, Calabrò A, Rizzo A, Annunziata S, et al. 18F-FDG PET/CT maximum tumor dissemination (Dmax) in lymphoma: a new prognostic factor? Cancers (Basel). 2023;15(9):2494. https://doi.org/10.3390/cancers15092494.
16. Aksu A, Vural Topuz Ö, Yılmaz G, Çapa Kaya G, Yılmaz B. Dual time point imaging of staging PSMA PET/CT quantification; spread and radiomic analyses. Ann Nucl Med. 2022;36(3):310–8. https://doi.org/10.1007/s12149-021-01705-5.
17. Aksu A, Vural Topuz Ö, Yilmaz B, Karahan Şen NP, Acar E, Çapa KG. Prediction of early biochemical response after 177Lu-PSMA radioligand therapy with 68Ga-PSMA PET, a different perspective with quantitative parameters. Nucl Med Commun. 2022;43(4):468–74. https://doi.org/10.1097/MNM.0000000000001539.
18. Nioche C, Orlhac F, Boughdad S, Reuzé S, Goya-Outi J, Robert C, et al. LIFEx: a freeware for radiomic feature calculation in multimodality imaging to accelerate advances in the characterization of tumor heterogeneity. Cancer Res. 2018;78(16):4786–9. https://doi.org/10.1158/0008-5472.CAN-18-0125.
19. Rowe SP, Pienta KJ, Pomper MG, Gorin MA. PSMA-RADS version 1.0: a step towards standardizing the interpretation and reporting of psma-targeted PET imaging studies. Eur Urol. 2018;73(4):485–7. https://doi.org/10.1016/j.eururo.2017.10.027.
20. Albano D, Bertoli M, Battistotti M, Rodella C, Statuto M, Giubbini R, et al. Prognostic role of pretreatment 18F-FDG PET/CT in primary brain lymphoma. Ann Nucl Med. 2018;32(8):532–41. https://doi.org/10.1007/s12149-018-1274-8.
21. Albano D, Bianchetti N, Talin A, Dondi F, Re A, Tucci A, et al. Prognostic role of pretreatment tumor burden and dissemination features from 2-[18F]FDG PET/CT in advanced mantle cell lymphoma. Hematol Oncol. 2025;43(1): e70009. https://doi.org/10.1002/hon.70009.
22. Albano D, Ravanelli M, Durmo R, Vesari A, Filice A, Rizzo A, et al. Semiquantitative 2-[18F]FDG PT/CT-based parameters role in lymphoma. Front Med. 2024. https://doi.org/10.3389/fmed.2024.1515040.
23. Schmuck S, von Klot CA, Henkenberens C, Sohns JM, Christiansen H, Wester HJ, et al. Initial experience with volumetric 68Ga-PSMA I&T PET/CT for assessment of whole-body tumor burden as a quantitative imaging biomarker in patients with prostate cancer. J Nucl Med. 2017;58(12):1962–8. https://doi.org/10.2967/jnumed.117.193581.
24. Brito AET, Mourato FA, de Oliveira RPM, Leal ALG, Filho PJA, de Filho JLL. Evaluation of whole-body tumor burden with 68Ga-PSMA PET/CT in the biochemical recurrence of prostate cancer. Ann Nucl Med. 2019;33(5):344–50. https://doi.org/10.1007/s12149-019-01342-z.
25. Schmidkonz C, Cordes M, Goetz TI, Prante O, Kuwert T, Ritt P, et al. 68Ga-PSMA-11 PET/CT derived quantitative volumetric tumor parameters for classification and evaluation of therapeutic response of bone metastases in prostate cancer patients. Ann Nucl Med. 2019;33(10):766–75. https://doi.org/10.1007/s12149-019-01387-0.
26. Alberts IL, Seide SE, Mingels C, Bohn KP, Shi K, Zacho HD, et al. Comparing the diagnostic performance of radiotracers in recurrent prostate cancer: a systematic review and network meta-analysis. Eur J Nucl Med Mol Imaging. 2021;48(9):2978–89. https://doi.org/10.1007/s00259-021-05210-9.

Publisher's Note Springer Nature remains neutral with regard to jurisdictional claims in published maps and institutional affiliations.

Annals of Hematology (2024) 103:2419–2427
https://doi.org/10.1007/s00277-024-05672-5

RESEARCH

2-[^{18}]F FDG PET/CT dissemination features in adult burkitt lymphoma Are predictive of outcome

Domenico Albano[1,2] · **Anna Calabrò**[1,2] · **Anna Talin**[1,2] · **Francesco Dondi**[1,2] · **Chiara Pagani**[3] · **Alessandra Tucci**[3] · **Giorgio Treglia**[4,5,6] · **Francesco Bertagna**[1,2]

Received: 28 December 2023 / Accepted: 17 February 2024 / Published online: 20 February 2024
© The Author(s), under exclusive licence to Springer-Verlag GmbH Germany, part of Springer Nature 2024

Abstract

This retrospective study investigated the prognostic role of disease dissemination features (Dmax and $Dmax_{bsa}$) measured by 2-[^{18}F]FDG PET/CT in newly diagnosed Burkitt Lymphoma (BL) patients, comparing their performance with other metabolic parameters. We included 78 patients diagnosed with BL between 2010 and 2022 with an available baseline PET, interim PET/CT (iPET) and end of treatment PET/CT (eotPET) and with a minimum of two 2-[^{18}F]FDG avid lesions present at the baseline scan. Dmax was calculated from the three-dimensional coordinates of the baseline metabolic tumor volume (MTV) by using LIFEx software; $Dmax_{bsa}$ was calculated as Dmax normalized for body surface area according to the Du Bois method. We evaluated their effect on metabolic treatment response evaluated by PET, on progression free survival (PFS) and on overall survival (OS). $Dmax_{bsa}$ was significantly associated with tumor stage, bulky and extranodal disease, MTV and TLG. At a median follow-up of 49 months, the median PFS and OS were 45 and 48 months. Dmax and $Dmax_{bsa}$ were significantly higher in not complete metabolic response than complete metabolic response group at iPET and eotPET.As far as PFS, parameters including iPET/CT, eotPET/CT outcomes, MTV and TLG showed to be independent prognostic factors while Dmax and $Dmax_{bsa}$ were not significantly associated with the outcome. Dissemination features, together with eotPET/CT results, MTV and TLG, demonstrated to be significantly correlated with OS. In conclusion, in this study we demonstrated that dissemination features derived by 2[^{18}F]-FDG PET/CT were significantly correlated with response to treatment and long-term outcome, independently from other PET features.

Keywords Burkitt lymphoma · PET/CT · Dmax · 18F-FDG · Nuclear medicine · Lymphoma

Introduction

Burkitt's lymphoma (BL) is a highly aggressive B-cell lymphoma that especially affects children and adolescents but accounts for only 1 to 2% of non-Hodgkin's lymphomas (NHL) in adults [1, 2]. BL typically has a dramatic clinical presentation, which warrants immediate evaluation, given the characteristically rapid growth of the lymphoma and spread to extranodal anatomical sites, including intraabdominal organs and the central nervous system. A high index of clinical suspicion is required for prompt diagnosis and early initiation of supportive care. Several studies demonstrated the viral role in tumor development and the hallmark translocation of the MYC oncogene, while genomic studies have shown the presence of mutations in p53 and along the phosphatidylinositol 3-kinase (PI3K) signaling pathway that contribute to oncogenesis [3, 4]. Although most patients are cured with intensive combination chemotherapy, given

✉ Domenico Albano
doalba87@libero.it

1 Nuclear Medicine, ASST Spedali Civili Brescia, Brescia 25123, Italy

2 Nuclear Medicine, University of Brescia, Brescia, Italy

3 Division of Hematology, ASST Spedali Civili Brescia, Brescia, Italy

4 Clinic of Nuclear Medicine, Imaging Institute of Southern Switzerland, Ente Ospedaliero Cantonale, Bellinzona, Switzerland

5 Faculty of Biology and Medicine, University of Lausanne, Lausanne, Switzerland

6 Faculty of Biomedical Sciences, Università Della Svizzera Italiana, Lugano, Switzerland

the paucity of randomized trials, optimal therapy has not been defined. Furthermore, treatment of elderly patients, patients with central nervous system involvement, or those with relapsed disease remains an unmet need. Adults are more susceptible to toxic effects but are effectively treated with chemotherapy, including modified versions of paediatric regimens. The outcomes in patients with BL are good in high-income countries with low mortality and few late effects, but in low-income and middle-income countries, BL is diagnosed late and is usually treated with less-effective regimens affecting the overall good outcome in patients with this lymphoma [5, 6].

Considering the high cell turnover and high aggressiveness of BL, it can be considered a fluorine-18-fluorodeoxyglucose (2-[^{18}F]FDG)-avid NHL subtype [7]. However, the effective potential usefulness of fluorine-18-fluorodeoxyglucose positron emission tomography/computed tomography (2-[^{18}F]FDG PET/CT) in the evaluation of BL patients is still under debate with promising evidence about staging and restaging [8–11], but not enough evidence on prognostic evaluation [12–14]. For these reasons, the identification of new prognostic not-invasive biomarkers seems to be crucial. Recently, a new PET-derived parameter was introduced for studying lymphomas and predicting their outcome: the maximum tumor dissemination (Dmax) [15, 16]. It was defined as the maximum distance between the two farthest hypermetabolic lesions using 2-[^{18}F]FDG PET/CT [15].

However, to the best of our knowledge, no previous studies have investigated the role of disease dissemination PET features in predicting treatment response and prognostication in BL.

Therefore, this retrospective study aimed to investigate the usefulness of dissemination PET features in predicting the outcome in adult patients affected by BL and to compare their performance with the other metabolic parameters.

Materials and methods

Patients

This research was a monocentric retrospective study. We included patients with histologically confirmed BL diagnosed in our hospital between January 2010 and January 2022, who had available baseline 2-[^{18}F]FDG PET/CT (bPET/CT), interim 2-[^{18}F]FDG PET/CT (iPET/CT) and end of treatment 2-[^{18}F]FDG PET/CT (eotPET/CT) with a minimum follow-up of 12 months from diagnosis. Only patients with a minimum of two hypermetabolic lesions at PET/CT were included. IPET was performed after 2–3 cycles of chemotherapy, while eotPET was performed after 6 cycles or prior to that if patients developed side effects that suggested interrupting the chemotherapy regimen.

For each patient, the main epidemiological (gender, age, immune system status), clinical (IPI score, Ann Arbor stage, presence of B symptoms, LDH level at diagnosis, type of treatment), morphological (presence of bulky disease) and PET/CT features were recorded. To define bulky disease, we considered any mass measuring 10 cm or more in diameter by any imaging study, or with a diameter equal or greater than one third of the internal transverse diameter of the thorax.

All patients were treated according to the institution's standard protocol with a chemotherapy regimen in use at the time of diagnosis. Sixty-four patients were treated according to the GMALL-B-ALL/NHL 2002 protocol [17] which includes six cycles of immunochemotherapy including methotrexate, cytosine arabinoside, cyclophosphamide, etoposide, ifosphamide, vincristine, adriamycin and rituximab-corticosteroids alternating every 3 or 4 weeks followed by two additional courses of rituximab afterwards. Six patients were treated with R-CHOP (rituximab plus cyclophosphamide, doxorubicin, vincristine, and prednisone) regimen. The remaining 2 patients received short-term intensified chemo-immunotherapy (rituximab, vincristine, etoposide, doxorubicin, methotrexate, cytarabine, prednisone) according to CARMEN regimen [18]. Six patients passed away before performing iPET.

2-[^{18}F]FDG PET/CT imaging and interpretation

2-[^{18}F]FDG PET/CT scanning was performed according to international guidelines [19]. The I.v. injection of 2-[^{18}F]FDG (activity: 3.5–4.5 Mbq/Kg) was performed after a minimum of 6 h fasting period and with blood glucose levels lower than 150 mg/dL. PET/CT was acquired about 60 min after the radiopharmaceutical injection. Acquisition was done from the skull basis to the mid-thigh. The tomographs available during patient's recruitment were a Discovery ST and a Discovery 690 (General Electric Company—GE®—Milwaukee, WI, USA) with standard parameters (CT: 80 mA, 120 Kv without contrast; 2.5–4 min per bed-PET-step of 15 cm; matrix of 128×128 or 256×256 and a field of view of 60 cm). bPET/CT was performed prior to any treatment and not earlier than 7 days prior to the first cycle of chemotherapy; iPET/CT was executed during the week before the third or fourth cycle (range 1–7 days) and eotPET/CT was performed at least 3 weeks after the completion of the last cycle of chemotherapy.

2-[^{18}F]FDG PET/CT scans for all patients were visually and semiquantitatively revised by two expert nuclear medicine physicians (DA; FD) who were blinded to the patient outcome.

2-[^{18}F]FDG PET/CT analysis

For qualitative analysis, every focal radiotracer uptake different from physiological distribution and background was considered 2-[^{18}F]FDG-avid and suggestive of disease. IPET and eotPET scans were classified according to Deauville Score (DS) and interpreted according to Lugano criteria [20, 21].

For semiquantitative analysis, we derived the maximum standardized uptake value body weight (SUVbw), maximum standardized uptake value lean body mass (SUVlbm), maximum standardized uptake value body surface area (SUVbsa), metabolic tumor volume (MTV), total lesion glycolysis (TLG), and Dmax. MTV was calculated in bPET using LIFEx software [22] and defined using the 41% SUVmax threshold. TLG was subsequently calculated mathematically as the sum of MTV*SUVmean for each lesion. Bone marrow involvement was included in the volume measurement only if there was focal uptake. To calculate Dmax, LIFEx software applying the Euclidean formula measured the distance between all pairs of lesions (including both nodal and extra nodal) recording the greatest lesion distance. Subsequently, Dmax was normalized by the patient body surface area (BSA) calculated according to the Du Bois method to get $Dmax_{bsa}$ [23].

Statistical analysis

The software used for the statistical analysis was MedCalc version 18 for Windows (Ostend, Belgium). The categorical variables were described as simple and relative frequencies, the numeric variables were described as average, standard deviations (SD) and range.

The relationship between $Dmax_{bsa}$ and the other clinical, pathological and metabolic parameters were calculated using the Kruskal-Wallis test and the Mann–Whitney U test. Variables for which p-value < 0.05 in univariate analysis were subjected to multiple linear regression analysis to determine those that were independently associated with semi-quantitatively features.

The optimal metabolic variables cut-off values for PFS and OS were determined using receiver operating curve (ROC) analysis. The cut-off values were chosen as the values maximizing the Youden index defined as the sum of sensitivity and specificity minus one (Supplemental Table 1).

Overall survival (OS) and progression free survival (PFS) were estimated with Kaplan-Meier curves and log-rank test was used to assess statistical significance. Coxproportional-hazards model was used for univariate and multivariate survival analysis.

OS was calculated from the date of baseline 2-[^{18}F]FDG PET/CT to the date of death from any cause or to the date of last follow-up. PFS was calculated from the date of baseline PET/CT to the date of first disease progression, relapse, death or the date of last follow-up.

Results

Patients and 2-[^{18}F]FDG PET/CT findings

Among 78 patients with histologically proven BL, 51 (65%) were male and 27 (35%) were female; average age was 52.8 years (range: 18–80 years). Patients were staged according to the Ann Arbor system as follows: stage II ($n = 22$), stage III ($n = 7$) and stage IV ($n = 49$). B-symptoms, bulky disease and extranodal localizations of lymphoma were present in 37, 27 and 44 cases, respectively. Most patients were immunocompetent ($n = 58$), while a state of immunodeficiency was described in 20 patients (HIV in 13 cases and post-transplant lymphoproliferative disease in 7 cases). IPI score was greater than 2 in 55 patients and LDH levels were higher than normal in 58 patients.

bPET/CT scans showed the presence of at least one lesion with increased 2-[^{18}F]FDG uptake in all 78 patients. Mean SUVbw of the hypermetabolic lesion was 16.6 (range 3.3–62); mean SUVlbm was 12.6 (range 2.4–41), mean SUVbsa 4.8 (range 0.9–17) mean MTV 387 cm^3 (6.1–3000 cm^3) and mean TLG was 408 (18–22,222) (Table 1).

Correlation between $Dmax_{bsa}$ and other variables

Average Dmax and $Dmax_{bsa}$ of the lesion with the highest uptake were 39.9 cm (range 3–92) and 22.3 cm (range 1.9–529) respectively (Fig. 1). In the univariate analysis, $Dmax_{bsa}$ was significantly correlated with tumor stage, LDH levels, age, bulky disease, presence of extranodal disease, IPI score, MTV and TLG and no other features (Table 2). In the multivariate analysis, tumor stage, bulky disease, extranodal disease, MTV and TLG were confirmed to be significantly associated with $Dmax_{bsa}$ ($p < 0.001$, 0.015, 0.003, < 0.001 and 0.002, respectively) (Table 2).

Role of 2-[^{18}F]FDG PET/CT in predicting treatment response

Based on Lugano classification metabolic response categories [21, 22], at iPET/CT 46 patients had complete metabolic response and 26 patients had not complete metabolic response (25 partial metabolic response and one progression of disease), whereas at eotPET/CT 49 had complete response and 23 not complete metabolic response (14 partial response, 8 progression of disease and 1 stable disease).

Table 1 characteristics of the whole population

	Patients n (%)
Gender	
Female	27 (35%)
Male	51 (65%)
Age, mean ± SD (range)	52.8 ± 17 (18–80)
Tumor stage at diagnosis (Ann arbor)	
II	22 (28%)
III	7 (9%)
IV	49 (63%)
Presence of B-symptoms	37 (48%)
LDH level increased	58 (74%)
Presence of bulky disease	27 (35%)
Presence of extranodal disease	44 (56%)
Immunocompromised patients	20 (26%)
IPI score > 2	55 (70%)
SUVbw, mean ± SD (range)	16.6 ± 10.9 (3.3–62)
SUVlbm, mean ± SD (range)	12.6 ± 8 (2.4–41)
SUVbsa, mean ± SD (range)	4.8 ± 2.9 (0.9–17)
MTV cm^3, mean ± SD (range)	387 ± 586 (6.1–3000)
TLG, mean ± SD (range)	4208 ± 5320 (18-22222)
Dmax cm, mean ± SD (range)	39.9 ± 24.9 (3–92)
$Dmax_{bsa}$ cm, mean ± SD (range)	22.3 ± 13.7 (1.9–52)

SD: standard deviation; *LDH* lactate dehydrogenase, *IPI* International Prognostic Score; *SUV*: standardized uptake value; *bw*: body weight; *lbm*: lean body mass; *bsa*: body surface area; *MTV*: metabolic tumor volume; *TLG*: total lesion glycolysis; *Dmax*: maximum tumor dissemination

Dmax and $Dmax_{bsa}$ were significantly higher in not complete metabolic response than complete metabolic response group at interim ($p = 0.009$ and $p = 0.004$), while no other metabolic variables (SUVbw, SUVlbm, SUVbsa, MTV and TLG) were significantly related with interim PET response (Table 3).

Baseline Dmax and $Dmax_{sba}$ in patients with complete metabolic response at iPET were 35.1 and 18.83 cm, while in patients without complete metabolic response were 45.5 and 25.4 cm, respectively.

Dmax and $Dmax_{bsa}$ were also significantly correlated with eotPET response. Baseline Dmax and $Dmax_{bsa}$ in patients with complete metabolic response at iPET were 32.07 and 17.43 cm, while in patients without complete metabolic response were 52.84 and 29.2 cm, respectively ($p < 0.001$). MTV and TLG were significantly lower in patients with complete metabolic response.

Other metabolic PET/CT features, as SUVbw, SUVlbm, SUVbsa, showed no statistically significant difference among complete response and not complete response group at end of treatment.

Role of 2-[^{18}F]FDG PET/CT in predicting progression free survival and overall survival

At a median follow-up of 49 months, relapse or progression of disease occurred in 23 patients with an average time of

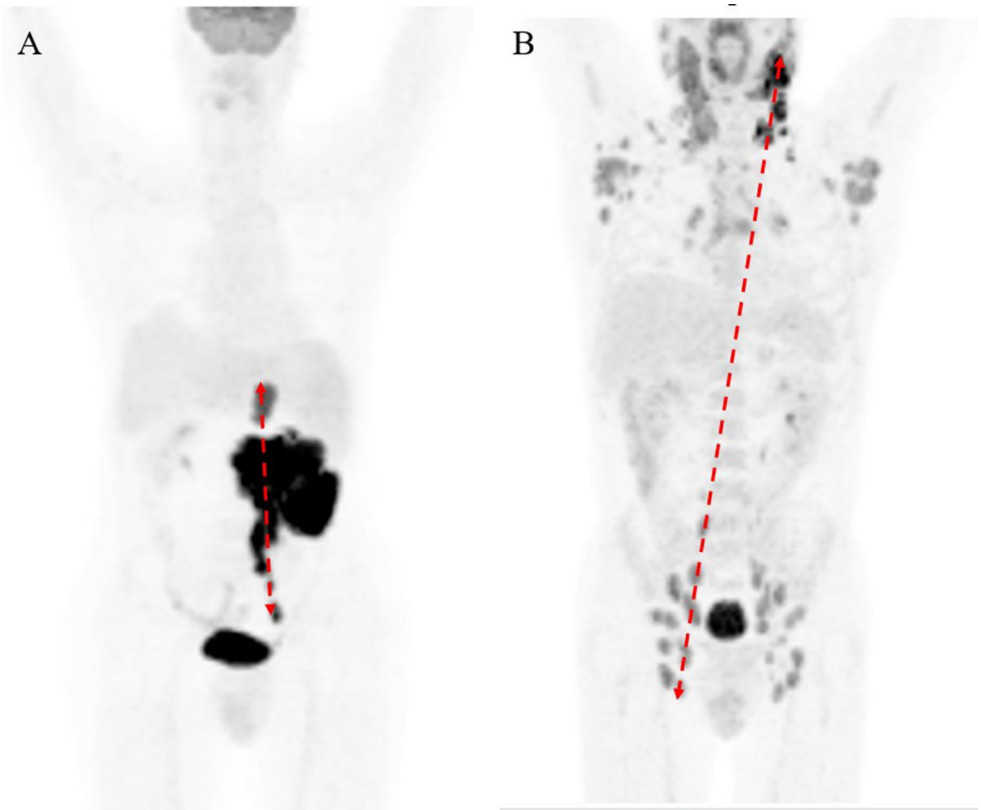

Fig. 1 An example of two patients with similar MTV values, but different Dmax and $Dmax_{bsa}$. (**A**) Stage II patient with MTV = 580 cm^3, Dmax = 16.4 cm and $Dmax_{bsa}$ = 9.16 cm. (**B**) Stage III patient with MTV = 550 cm^3, Dmax = 73.8 cm and $Dmax_{bsa}$ = 42.9 cm

Table 2 comparison between $Dmax_{bsa}$ and clinical-pathological variables in BL patients

	$Dmax_{bsa}$, average	p value (univariate)	p value (multivariate)
Gender		0.315	
Male	21.7		
Female	24.1		
Age		0.009	0.125
Stage acc Ann Arbor		< 0.001	< 0.001
II	10.6		
III	22.6		
IV	27.6		
B symptoms		0.319	
Present	25.1		
Not present	20.2		
LDH level		0.329	
Normal	22.5		
Increased	24.8		
Bulky disease		0.008	0.015
Present	19.3		
Not present	25.3		
Extranodal disease		< 0.001	0.003
Present	27.4		
Not present	16.2		
Immunocompromised		0.797	
Yes	24.4		
No	21.8		
IPI score		0.042	0.096
≤2	19		
>2	26.9		
MTV		< 0.001	< 0.001
≤228	15.4		
>228	31.4		
TLG		< 0.001	0.002
≤1263	15.8		
>1263	27.5		
SUVbw		0.353	
≤9.2	19.5		
>9.2	23.3		
SUVlbm		0.549	
≤7.8	20.5		
>7.8	23.3		
SUBbsa		0.522	
≤3.1	20.3		
>3.1	23.6		

LDH lactate dehydrogenase, *IPI* International Prognostic Score, *SUV*: standardized uptake value; *bw*: body weight; *lbm*: lean body mass; *bsa*: body surface area; *MTV*: metabolic tumor volume; *TLG*: total lesion glycolysis; *Dmax*: maximum tumor dissemination

19 months (range: 3–82 months) from bPET/CT and death occurred in 27 patients with an average time of 25.2 months (range 4-145 months). The median PFS was 45 months (range 2-154 months) and the median OS was 48.4 months (range 2–154 months). The estimated 3-year PFS and OS rates were 67% and 66%, respectively, while 5-year PFS and OS rates were 54% and 52%, respectively.Concerning PFS, iPET/CT, eotPET/CT results, MTV, TLG, Dmax and $Dmax_{bsa}$ were significantly correlated with the risk of progression/relapse at univariate analysis., iPET/CT, eotPET/CT results, MTV and TLG were confirmed to be independent prognostic factors at multivariate analysis while Dmax and $Dmax_{bsa}$ resulted no significantly associated with the outcome (Table 4) (Fig. 2).

Concerning OS, only eotPET/CT results, MTV, TLG, Dmax and $Dmax_{bsa}$ were significantly associated with outcome at univariate analysis. All these variables were confirmed to be independent prognostic factors at multivariate analysis ($p = 0.041$, $p = 0.001$, $p = 0.047$, $p = 0.001$, $p < 0.001$, respectively) (Table 4) (Fig. 3).

Discussion

The early and accurate identification of patients who failed to be cured is a milestone to enable testing of alternative treatments in BL. This requires a reliable risk stratification model and 2-[^{18}F]FDG PET/CT and its features may have a key-role. The prognostic role of MTV and TLG in predicting treatment response and prognosis in lymphomas, and also in BL, has already been demonstrated [14, 24], but several methodological concerns are still at play.

Moreover, the heterogeneity of the distribution, the distance between lesions and the number of lesions is not considered with MTV and TLG measurements. BL usually involves multiple disseminated nodal sites often associated with extranodal sites (such as central nervous system and bone tissue), sometimes with mutational heterogeneity impacting outcome. For these reasons, the introduction of a parameter that describes the tumor distribution and dissemination could be interesting and of clinical impact. Several studies demonstrated that a high Dmax was significantly correlated with poor prognosis, independently of MTV; the combination of MTV and Dmax seemed to increase the prognostic performance of 2-[^{18}F]FDG PET/CT even more [16].

First, Cottereau et al. [15] studied a cohort of 95 patients with an advanced stage DLBCL and showed that Dmax was an independent prognostic factor for PFS and OS, and the model combining MTV and Dmax was demonstrated to be effective at stratifying patients with higher accuracy than Ann Arbor classification. In our research, $Dmax_{ssa}$ and MTV showed to be superior than Ann Arbor stage in the prognostic field. In fact, Ann Arbor stage, resulted not significantly associated with both PFS and OS. Thus, $Dmax_{bsa}$ which intuitively reflects the dissemination of the disease, outperformed Ann Arbor stage for prognostication

Table 3 Comparison of metabolic PET/CT features between partial response and complete response groups at interim and end-of-treatment

Parameter (mean)	Interim response		p value	End of treatment response		p value
	Complete response	Not complete response		Complete response	Not complete response	
SUVbw	15.85	18.85	0.281	14.97	20.94	0.093
SUVlbm	11.88	14.56	0.199	11.76	14.93	0.132
SUVbsa	4.60	5.48	0.280	4.46	5.85	0.060
MTV	353.6	461	0.478	321	538.3	0.015
TLG	4040	4775	0.592	3535	5892	0.008
Dmax	35.1	45.5	0.009	32.07	52.84	< 0.001
$Dmax_{bsa}$	18.83	25.4	0.004	17.43	29.2	< 0.001

SUV: standardized uptake value; *bw*: body wheight; *lbm*:lean body mass; *bsa*: body surface area; *MTV*: total metabolic tumor volume; *TLG*: total lesion glycolysis; *Dmax*: maximum tumor dissemination

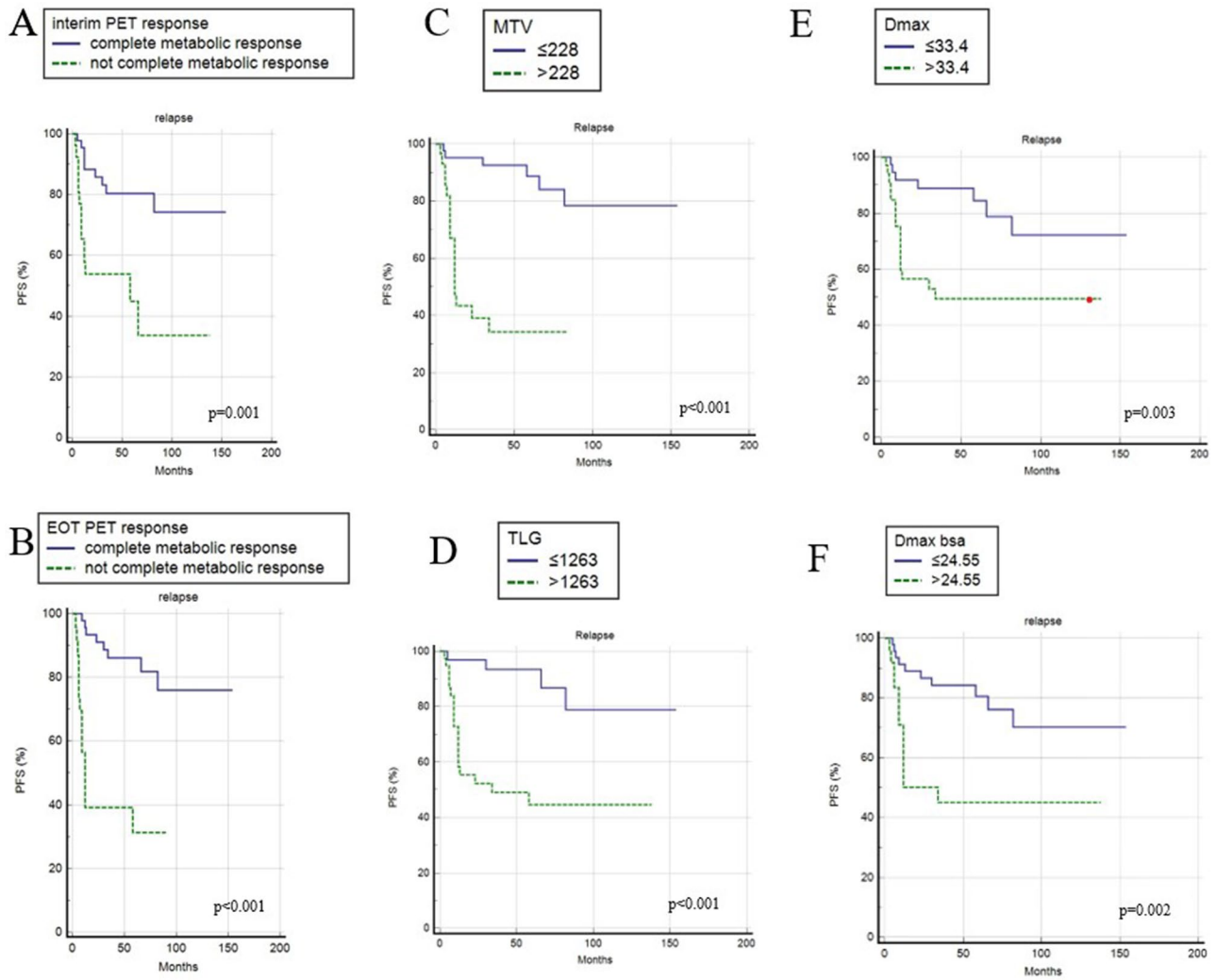

Fig. 2 Progression-free survival curves of interim PET/CT response (**A**), end of treatment PET/CT response (**B**), MTV (**C**), TLG (**D**), Dmax (**E**) and $Dmax_{bsa}$ (**F**)

and therefore remained relevant even among patients with advanced disease.

In this study we decided to also evaluate Dmax normalized by BSA in order to take into account the size and height of each patient, yielding the $Dmax_{bsa}$. This normalization was suggested previously by other groups [25, 26], but it is not yet globally shared. We believed that body composition features may influence the effective measurement of Dmax affecting the potential extraction of thresholds.

Table 4 univariate and multivariate analyses for PFS and OS

	Univariate analysis		Multivariate analysis	
	p value	HR (95% CI)	p value	HR (95% CI)
PFS				
Sex	0.350	1.600 (0.696–3.999)		
Tumor Stage	0.222	0.670 (0.234–1.299)		
IPI score	0.555	1.567 (0.500-2.001)		
LDH level	0.601	0.879(0.256–3.301)		
Bulky disease	0.099	0.489 (0.401–1.125)		
Immune system condition	0.380	0.600 (0.303–2.580)		
Interim PET response	0.001	4.538 (1.829–11.254)	0.030	3.033 (1.110–8.288)
Eot PET response	< 0.001	11.927 (4.418–32.195)	0.024	2.822 (1.023–7.806)
SUVbw	0.056	2.317(0.219–1.408)		
SUVlbm	0.251	1.769 (0.976-5.500)		
SUVbsa	0.127	1.956 (0.825–4.634)		
MTV	< 0.001	9.813 (3.876–24.843)	0.001	6.017 (1.946–18.607)
TLG	< 0.001	4.739 (2.046–10.974)	0.018	3.963 (1.262–12.439)
Dmax	0.003	3.511 (1.499–8.221)	0.290	2.130 (0.524–8.653)
$Dmax_{sba}$	0.002	4.268 (1.687–10.780)	0.526	0.626 (0.147–2.662)
OS				
Sex	0.358	1.958 (0.401–5.859)		
Tumor Stage	0.250	0.348 (0.158–1.255)		
IPI score	0.658	0.698 (0.505–3.125)		
LDH level	0.787	2.0250 (0.401–4.150)		
Bulky disease	0.150	0.448 (0.303–2.268)		
Immune system condition	0.888	1.250 (0.199–2.590)		
Interim PET response	0.304	1.659 (0.631–4.360)		
Eot PET response	0.014	3.817 (1.304–11.168)	0.041	2.121 (1.333–3.356)
SUVbw	0.113	1.894 (0.589–4.176)		
SUVlbm	0.146	1.805 (0.813–4.018)		
SUVbsa	0.076	2.032 (0.926–4.457)		
MTV	< 0.001	10.287 (4.325–24.466)	0.001	5.698 (1.023–9.857)
TLG	< 0.001	4.878 (2.230-10.669)	0.047	2.250 (1.120–4.021)
Dmax	< 0.001	4.487 (2.061–9.769)	0.001	3.176 (1.146–8.795)
$Dmax_{sba}$	< 0.001	7.847 (3.375–18.261)	< 0.001	5.000 (1.500-10.201)

PFS: progression free survival; *OS*: overall survival; *HR*: hazard ratio; *CI*: confidence interval; *SUV*: standard uptake value; *bw*: body weight; *lbm*: lean body mass; *bsa*: body surface area; *MTV*: metabolic tumor volume; *TLG*: total lesion glycolysis; *LDH* lactate dehydrogenase, *IPI* International Prognostic Score

*Variables dichotomized using thresholds values after ROC analysis reported in Supplemental Table 1

An advantage of Dmax measure compared to other PET variables (MTV and TLG) is the relative simplicity and speed of measurement, now automated, and the clinical meaning of this parameter expression of patient-based spatial migration of disease.This metric is deeply different from complex radiological features that are usually difficult to explain from a biological perspective, such as radiomics features. Moreover, this parameter does not seem to be affected by PET/CT scanner performanceand scanning protocols, like SUV.

Larger studies are needed to determine the best combination of prognostic factors and the factors most readily used in clinical practice for lymphoma.

In other words, dissemination features are parameters that may express the dissemination/spread of disease in the whole body. However, despite promising results, a shared consensus about the best way to measure Dmax is unclear. In several studies, it was considered as absolute value without any correction related to the body composition of the patient [16].

In our study, Dmax, $Dmax_{bsa}$. MTV and TLG had an independent predictive value. We could hypothesize a prognostic scoring system based on these features extracted from the baseline PET/CT scan that are complementary as they characterize two different features of the disease: tumor burden and its dissemination. This score could potentially be more beneficial for patient risk stratification in guiding therapy than the current Ann Arbor staging system, which failed to predict outcome in this cohort, or the current prognostic indices such as IPI. We did not test this score in our population due to the low sample of patients included.

Of course, further studies on larger cohorts would be useful in supporting or challenging our preliminary findings.

Another fundamental finding of our paper is the confirmation of the prognostic role of metabolic response at interim and end of treatment. IPET and eotPET results are significantly associated with PFS, while only eotPET is

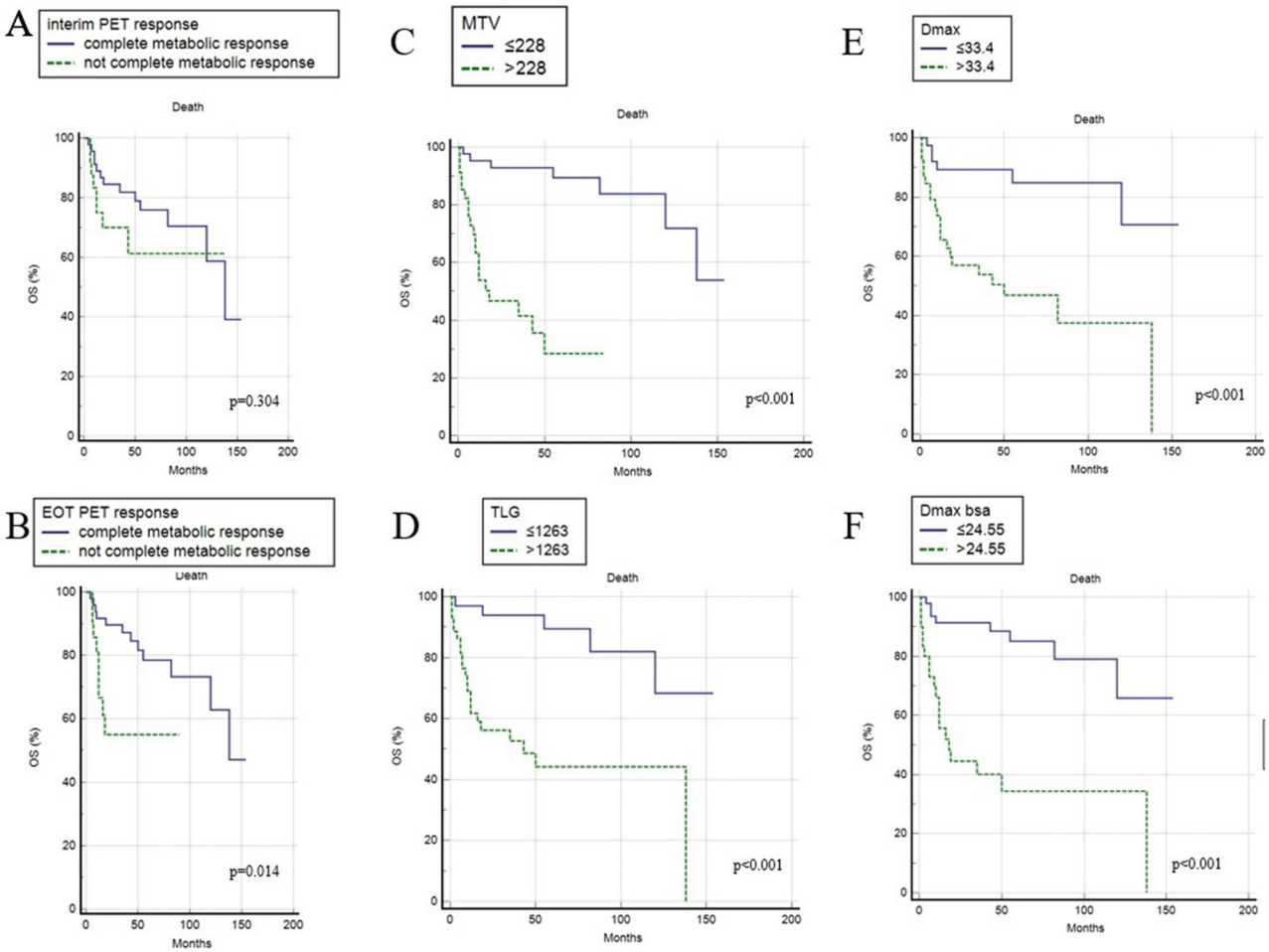

Fig. 3 Overall survival curves of interim PET/CT response (**A**), end of treatment PET/CT response (**B**), MTV (**C**), TLG (**D**), Dmax (**E**) and $Dmax_{bsa}$ (**F**)

related to OS. These results are concordant with previous evidence [26, 27]. The Lugano recommendations routinely recommend 2-[^{18}F]FDG PET/CT before and after treatment in tracer avid lymphomas, like HL and DLBCL [20, 21], but the definition of 2-[^{18}F]FDG -avid lymphomas is constantly evolving. Despite the low number of available scans, also BL seems to be 2-[^{18}F]FDG-avid in most cases probably due to the aggressiveness of the disease [28–30].

This study had the following limitations: first, its retrospective nature; second, the patients small sample size; third, the long period of inclusion of patients; fourth, the heterogeneity of treatments regimen.

Conclusion

In conclusion, in this study we demonstrated that dissemination features derived by 2-[^{18}F]FDG PET/CT were significantly correlated with response to treatment and long-term outcome, independently from other PET features.

Supplementary Information The online version contains supplementary material available at https://doi.org/10.1007/s00277-024-05672-5.

Author contributions Conceptualization, D.A. and A.C.; methodology, G.T. and F.D.; data curation, A.T.; A.C.; C.P. and F.D.; supervision,A.T. and F.B.; writing—original draft preparation, D.A., G.T. and A,C. Preparation figures: C.P., A.T., F.D. All authors have read and agreed to the published version of the manuscript.

Funding No funding.

Data availability No datasets were generated or analysed during the current study.

Declarations

Ethical approval Ethical approval: all procedures performed in studies involving human participants were in accordance with the ethical standards of the institutional and/or national research committee and with the 1964 Helsinki declaration and its later amendments or comparable ethical standards. Ethical review and approval were waived for this study (observational retrospective) due to the retrospective design of the study, according to local laws.

Competing interests The authors declare no competing interests.

References

1. Teras LR, DeSantis CE, Cerhan JR, Morton LM, Jemal A, Flowers CR (2016) 2016 US lymphoid malignancy statistics by World Health Organization subtypes. CA Cancer J Clin 66:443–459
2. Roschewski M, Staudt LM, Wilson WH (2022) Burkitt's lymphoma. N Engl J Med 387(12):1111–1122. https://doi.org/10.1056/NEJMra2025746
3. Schmitz R, Young RM, Ceribelli M et al (2012) Burkitt lymphoma pathogenesis and therapeutic targets from structural and functional genomics. Nature 490(7418):116–120. https://doi.org/10.1038/nature11378
4. Grande BM, Gerhard DS, Jiang A et al (2019) Genome-wide discovery of somatic coding and noncoding mutations in pediatric endemic and sporadic Burkitt lymphoma. Blood 133(12):1313–1324. https://doi.org/10.1182/blood-2018-09-871418
5. Crombie J, LaCasce A (2021) The treatment of Burkitt lymphoma in adults. Blood 137(6):743–750. https://doi.org/10.1182/blood.2019004099
6. López C, Burkhardt B, Chan JKC et al (2022) Nat Rev Dis Primers 8(1):78. https://doi.org/10.1038/s41572-022-00404-3
7. Albano D, Bertagna F, Giubbini (2020) R.18F-FDG PET/CT role in Burkitt lymphoma. Clin Transl Imaging 8:39–45
8. Just PA, Fieschi C, Baillet G et al (2008) 18F-fluorodeoxyglucose positron emission tomography/computed tomography in AIDS-related Burkitt lymphoma. AIDS Patient Care STDS 22:695–700
9. Zeng W, Lechowicz MJ, Winton E et al (2009) Spectrum of FDG PET/CT findings in Burkitt lymphoma. Clin Nucl Med 4:355–358
10. Karantanis D, Durski JM, Lowe VJ et al (2012) 18F-FDG PET and PET/CT in Burkitt's lymphoma. Eur J Radiol 75:e68–73
11. Carrillo-Cruz E, Rodrıguez MS, Borrego-Dorado I et al (2015) Role of 18F-FDG-PET/CT in the management of Burkitt lymphoma. Eur J Haematol 94:23–30
12. Albano D, Bosio G, Re A et al (2018) Metabolic behaviour and prognostic value of early and end of treatment 18F-FDG PET/CT in adult Burkitt lymphoma: role of Deauville and IHP criteria. Leuk Lymphoma 3:1–8
13. Wei WX, Huang JJ, Li WY et al (2015) Prognostic values of interim and post-therapy 18F-FDG PET/CT scanning in adult patients with Burkitt's lymphoma. Chin J Cancer 2(34):608–613
14. Albano D, Bosio G, Pagani C et al (2019) Prognostic role of baseline 18F-FDG PET/CT metabolic parameters in Burkitt lymphoma. Eur J Nucl Med Mol Imaging 46:87–96
15. Cottereau AS, Nioche C, Dirand AS, Clerc J, Morschhauser F, Casasnovas O, Meignan M, Buvat I (2020) 18F-FDG PET dissemination features in diffuse large B-Cell lymphoma are Predictive of Outcome. J Nucl Med 61(1):40–45. https://doi.org/10.2967/jnumed.119.229450
16. Albano D, Treglia G, Dondi F, Calabrò A, Rizzo A, Annunziata S, Guerra L, Morbelli S, Tucci A, Bertagna F (2023) 18F-FDG PET/CT maximum tumor dissemination (Dmax) in lymphoma: a New Prognostic factor? Cancers (Basel). 15(9):2494. https://doi.org/10.3390/cancers15092494
17. Hoelzer D, Walewski J, Döhner H, Viardot A, Hiddemann W, Spiekermann K et al (2014) Improved outcome of adult Burkitt lymphoma/leukemia with rituximab and chemotherapy: report of a large prospective multicenter trial. Blood 124:3870–3879
18. Ferreri AJ, Bruno VM, Donadoni G, Cattaneo C, Fumagalli L, Foppoli M et al (2012) Safety and activity of a new intensive short-term chemoimmunotherapy in HIV-positive patients with Burkitt lymphoma. Br J Haematol 159:252–255
19. Boellaard R, Delgado-Bolton R, Oyen WJG et al (2015) FDG PET/CT: EANM procedure guidelines for tumour imaging: version 2.0. Eur J Nucl Med Mol Imag 42(2):328–354. https://doi.org/10.1007/s00259-014-2961-x
20. Cheson BD, Fisher RI, Barrington SF et al (2014) Recommendations for initial evaluation, staging, and response assessment of hodgkin and non-hodgkin lymphoma: the lugano classification. J Clin Oncol 32(27):3059–3067. https://doi.org/10.1200/jco.2013.54.8800
21. Barrington SF, Mikhaeel NG, Kostakoglu L, Meignan M, Hutchings M, Müeller SP et al (2014) Role of imaging in the staging and response assessment of lymphoma: consensus of the international conference on malignant lymphomas imaging working group. J Clin Oncol. ;32:3048–58
22. Nioche C, Orlhac F, Boughdad S et al (2018) LIFEx: a freeware for radiomic feature calculation in multimodality imaging to accelerate advances in the characterization of tumor heterogeneity. Cancer Res 78(16):4786–4789. https://doi.org/10.1158/0008-5472.CAN-18-0125
23. Dubois D, Dubois EF (1916) A formula to estimate the approximate surface area if height and weight be known. Arch Intern Med 17:863–871
24. Frood R, Burton C, Tsoumpas C, Frangi AF, Gleeson F, Patel C, Scarsbrook A (2021) Baseline PET/CT imaging parameters for prediction of treatment outcome in Hodgkin and diffuse large B cell lymphoma: a systematic review. Eur J Nucl Med Mol Imaging 48(10):3198–3220. https://doi.org/10.1007/s00259-021-05233-2
25. Durmo R, Donati B, Rebaud L, Cottereau AS, Ruffini A, Nizzoli ME, Ciavarella S, Vegliante MC, Nioche C, Meignan M, Merli F, Versari A, Ciarrocchi A, Buvat I, Luminari S (2022) Prognostic value of lesion dissemination in doxorubicin, bleomycin, vinblastine, and dacarbazine-treated, interimPET-negative classical Hodgkin Lymphoma patients: a radio-genomic study. Hematol Oncol 40(4):645–657. https://doi.org/10.1002/hon.3025
26. Cottereau AS, Meignan M, Nioche C, Capobianco N, Clerc J, Chartier L, Vercellino L, Casasnovas O, Thieblemont C, Buvat I (2021) Risk stratification in diffuse large B-cell lymphoma using lesion dissemination and metabolic tumor burden calculated from baseline PET/CT. Ann Oncol 32(3):404–411. https://doi.org/10.1016/j.annonc.2020.11.019
27. Bailly C, Eugène T, Couec ML, StrulluM, Frampas E, Campion L et al (2014) Prognostic value and clinical impact of (18)FDG-PET in the management of children with Burkitt lymphoma after induction chemotherapy. Front Med (Lausanne) 16(1):54
28. Wen WX, Huang JJ, Li WY, Zhang X, Xia Y, Jiang WQ et al (2015) Prognostic values of interim and post-therapy 18F-FDG PET/CT scanning in adult patients with Burkitt's lymphoma. Chin J Cancer 2(34):608–613
29. Zeng W, Lechowicz MJ, Winton E, Cho SM, Galt JR, Halkar R (2009) Spectrum of FDG PET/CT findings in Burkitt lymphoma. Clin Nucl Med 4:355–358
30. Karantanis D, Durski JM, Lowe VJ, Nathan MA, Mullan BP, Georgiou E et al (2012) 18F-FDG PET and PET/CT in Burkitt's lymphoma. Eur J Radiol 75:e68–73

Publisher's Note Springer Nature remains neutral with regard to jurisdictional claims in published maps and institutional affiliations.

Springer Nature or its licensor (e.g. a society or other partner) holds exclusive rights to this article under a publishing agreement with the author(s) or other rightsholder(s); author self-archiving of the accepted manuscript version of this article is solely governed by the terms of such publishing agreement and applicable law.

Journal of *Personalized Medicine*

MDPI

Article

Correlation between Kidney Uptake at [18F]FDG PET/CT and Renal Function

Francesco Dondi [1,†], Antonio Rosario Pisani [2,†], Nicola Maria Lucarelli [2], Maria Gazzilli [3,*], Anna Talin [1], Domenico Albano [1], Dino Rubini [4], Nicola Maggialetti [2], Giuseppe Rubini [2] and Francesco Bertagna [1]

1 Nuclear Medicine, Università Degli Studi di Brescia and ASST Spedali Civili Brescia, 25123 Brescia, Italy; f.dondi@outlook.com (F.D.); anna.talin@gmail.com (A.T.); domenico.albano@unibs.it (D.A.); francesco.bertagna@unibs.it (F.B.)
2 Section of Nuclear Medicine, Interdisciplinary Department of Medicine, University of Bari "Aldo Moro", Piazza Giulio Cesare 11, 70124 Bari, Italy; antoniorosario.pisani@uniba.it (A.R.P.); nicola.maggialetti@uniba.it (N.M.); giuseppe.rubini@uniba.it (G.R.)
3 Nuclear Medicine, ASL Bari—P.O. Di Venere, 70012 Bari, Italy
4 Department of Precision Medicine, University of Campania "L. Vanvitelli", 80138 Naples, Italy; dinoru95@hotmail.it
* Correspondence: marinagazzilli@msn.com
† These authors contributed equally to this work.

Abstract: Different insights into the connection between kidney [^{18}F]fluorodesoxyglucose ([^{18}F]FDG) uptake at positron emission tomography/computed tomography (PET/CT) and renal function have been proposed in the past. The aim of this study was therefore to assess the presence of a correlation between these two parameters. Kidney uptakes were assessed and compared to the creatinine (Cr) values and estimated glomerular filtration rate (EGFR) among different classes of renal functional impairment or kidney status. A total of 339 patients and 385 different PET/CT scans were included in this study. Significant correlations between kidney uptakes and renal function parameters were reported in most of the groups studied, with the exception of patients with Cr < 1.2 mg/dL and subjects with a kidney transplantation. Strong concordance in the assessment of renal parenchymal uptakes between the different readers was reported. To conclude, strong correlations for renal [^{18}F]FDG uptake with Cr levels and the EGFR were reported, with the exception of the group of patients with a Cr value < 1.2 mg/dL and for the group with a kidney transplantation.

Keywords: CKD; chronic kidney disease; PET/CT; positron emission tomography; [^{18}F]FDG

check for updates

Citation: Dondi, F.; Pisani, A.R.; Lucarelli, N.M.; Gazzilli, M.; Talin, A.; Albano, D.; Rubini, D.; Maggialetti, N.; Rubini, G.; Bertagna, F. Correlation between Kidney Uptake at [18F]FDG PET/CT and Renal Function. *J. Pers. Med.* **2024**, *14*, 40. https://doi.org/10.3390/jpm14010040

Academic Editor: Yong-An Chung

Received: 1 December 2023
Revised: 24 December 2023
Accepted: 28 December 2023
Published: 28 December 2023

Copyright: © 2023 by the authors. Licensee MDPI, Basel, Switzerland. This article is an open access article distributed under the terms and conditions of the Creative Commons Attribution (CC BY) license (https://creativecommons.org/licenses/by/4.0/).

1. Introduction

Chronic kidney disease (CKD) is a clinical syndrome caused by an irreversible change in renal function usually characterized by a slowly progressive evolution [1]. This condition has a higher prevalence in the adult population and is associated with different other pathological entities, such as an increased risk of cardiovascular disease and death [1]. Many different causes can contribute to the development of CKD; however, the most frequent are hypertension and diabetes, chronic glomerulonephritis or pyelonephritis, polycystic kidney disease, Alport's disease, autoimmune diseases, congenital malformations and the use of anti-inflammatory drugs [1,2].

CKD is diagnosed when an estimated glomerular filtration rate (EGFR) lower than 60 mL/min/1.73 m^2 has been present for at least three months or in the presence of an alteration in the renal structure. The disease can be classified into five different stages according to the impairment of the EGFR, which represents the rate at which the glomerulus filters plasma to produce urine and it is used to diagnose, stage and manage CKD [3]. These parameters cannot be measured directly so it is estimated based on the blood concentration of an endogenous filtration marker that is usually represented by creatinine (Cr), the most commonly used for this purpose [3]. Cr originates from muscle mass and diet through meat

proteins, is freely filtered by the glomerulus and also secreted by the renal tubules [3]. The Kidney Disease: Improving Global Outcomes (KDIGO) CKD guidelines recommend the use of the EGFR for the determination of the disease because of its simplicity, availability, cost-effectiveness and accuracy in predicting renal function in standard conditions. The estimating equation recommended by the KDIGO work group for the assessment of the EGFR in adults is the CKD Epidemiology Collaboration (CKD-EPI) [3,4].

[^{18}F]fluorodesoxyglucose ([^{18}F]FDG) positron emission tomography/computed tomography (PET/CT) is a hybrid imaging modality that in the last few years has been gaining more and more attention, due to its ability to evaluate a high amount of different conditions, both neoplastic or benign [5–7]. [^{18}F]FDG is a glucose analog able to identify tissues with high glycolytic activity and it is excreted by the kidneys with incomplete reabsorption in the proximal renal tubules [8]. Nevertheless, the usefulness of [^{18}F]FDG PET/CT for the assessment and the evaluation of different renal conditions has been reported in the past. Interestingly, it has been underlined that renal tissue is able to concentrate [^{18}F]FDG and that this uptake is related to the degree of sensitivity to insulin [9]. Moreover, a theoric model has been proposed that showed that the more severe the renal failure is, the more overestimated the standardized uptake value (SUV) is, unless the renal failure indirectly impairs tissue sensitivity to insulin and hence glucose metabolism [10]. Furthermore, some insights on the role of PET/CT imaging for the evaluation and the follow-up of renal allograft rejection and early evaluation of treatment response have been proposed in the literature [11–14]. PET/magnetic resonance (PET/MR) performed with [^{18}F]FDG also revealed a possible role to estimate renal function in terms of the EGFR and effective renal plasma flow (ERPF) [15]. Moreover, given the fact that, as mentioned, a higher cardiovascular risk is present in patients with CKD and that CKD is associated with myocardial metabolic changes, it has been reported that [^{18}F]FDG PET/CT could have the ability to investigate preclinical myocardial abnormalities in these patients [16]. Similarly, PET/CT was proposed as a valuable diagnostic tool for verifying and quantifying accelerated atherosclerosis secondary to CKD in patients on hemodialysis, with changes in tracer uptake that appeared to be accelerated in these subjects [17]. Interestingly, it has also been reported that [^{18}F]FDG PET/CT could assess the presence of inflammation in the carotid arteries, revealing therefore that renal transplantation may confer an anti-inflammatory effect on carotid atherosclerosis [18]. In addition, hybrid molecular imaging with [^{18}F]FDG is known to have high sensitivity for the evaluation of a wide range of inflammatory diseases and in this setting, it demonstrated its role for the diagnosis of the cause of fever of unknown origin (FUO) in CKD subjects on hemodialysis [19–21]. Similarly, PET/CT has also demonstrated its role for the evaluation of patients with autosomal dominant polycystic kidney disease and suspected cyst infection, with high diagnostic performances [22].

Some studies on the ability of CKD to modify the uptake of [^{18}F]FDG during a PET/CT scan have also been published with heterogeneous results. In some cases, it has been reported that the impairment of renal function does not significantly compromise the clearance of the background activity of [^{18}F]FDG in PET imaging [23]. In contrast, other papers instead observed that patients with CKD have a higher physiological tracer uptake in the liver and blood pool [24]. However, it has been demonstrated that CKD patients on hemodialysis show a significantly higher physiological [^{18}F]FDG uptake in the soft tissues, spleen and the blood pool compared to normal subjects [25]. Despite that, it was, however, suggested that CKD and subsequent renal failure do not require an adjustment in PET/CT protocols and that the standard protocol times should also be used in patients with renal failure [26].

The main purpose of our study was therefore to search for a possible correlation between renal uptake at [^{18}F]FDG PET/CT and renal functional parameters in both normal subjects and patients with CKD.

2. Materials and Methods

2.1. Patients Selection

In order to select patients suitable for inclusion in the present study, we retrospectively analyzed our databases to find subjects with CKD submitted to our center to undergo [^{18}F]FDG PET/CT for any reason. The interval time of this study was between January 2011 and May 2023. The exclusion criteria were as follows: (1) age under 18 years, (2) presence of pathological conditions affecting kidneys (e.g., cancers, inflammation, polycystic kidney disease) that made it impossible to assess kidney [^{18}F]FDG uptake, (3) absence of serum Cr values in the 7 days before or after the PET/CT scan and (4) presence of liver disease, affecting the value of the SUVmax. After applying such criteria, 224 patients with CKD were included. Moreover, 115 subjects without CKD who underwent [^{18}F]FDG PET/CT in our institution for various conditions were arbitrarily selected as the controls, with the same exclusion criteria mentioned before applied.

Ethical review and approval were waived for this study due to its retrospective design, according to local laws and to the ethics committees of our center. Informed consent was obtained from all individual participants included in this study. Information about gender and age was collected for all the subjects.

For all the patients included in this study, data about serum Cr levels and estimated glomerular filtration rate (EGFR) calculated with the CKD-EPI formula [3] were collected. Based on the EGFR, patients were also classified between the 5 stages of CKD. Moreover, in the case of patients undergoing different PET/CT scans, the evolution of these values at the time of the scan was also assessed and, in particular, dCr was calculated as the difference between the value of Cr at the second evaluation and the value at the first evaluation. Similarly, dEGFR was calculated as the difference between the EGFR at the time of the second PET/CT scan and the value at the first scan.

2.2. [^{18}F]FDG PET/CT Acquisition and Interpretation Protocol

A blood glucose level lower than 150 mg/dL was required for all the patients before undergoing [^{18}F]FDG PET/CT and they fasted for at least 6 hours before tracer injection. Patients voided before imaging acquisition, no oral or intravenous contrast agents were administrated or bowel preparation used for any patient. Blood glucose levels and the use of insulin replacement therapy at the moment of the scan were collected. An activity of 3.5–4.5 MBq/Kg of [^{18}F]FDG was intravenously administered and images were acquired at least 60 $\pm$ 10 min after injection from the skull basis to the mid-thigh on a Discovery ST or Discovery 690 PET/CT tomograph (General Electric Company, GE, Milwaukee, Wisconsin) with standard parameters (CT: 80 mA, 120 kV; PET: 2.5–4 min per bed position, PET step of 15 cm). Reconstructions were performed with a 256 $\times$ 256 matrix and a 60 cm field of view. On the Discovery 690 tomograph, time of flight (TOF) and point spread function (PSF) algorithm were used for the reconstruction of images, with filter cut-off 5 mm, 18 subsets and 3 iterations. For the Discovery ST tomograph, an ordered subset expectation maximization (OSEM) algorithm with filter cut-off 5 mm, 21 subsets and 2 iterations was applied.

PET/CT images were visually and semiquantitatively analyzed by two experienced nuclear medicine physicians. First of all, renal uptake for each kidney was calculated as the average of the SUVmax of 5 spheric volumes of interest (VOI) for each kidney, as presented in Figure 1. To obtain the total kidney uptake of a single patient (K), a mean of all its renal average uptakes was calculated. Moreover, the SUVmax of the liver was calculated using a spheric VOI with 1 cm diameter placed at the VIII hepatic segment from transaxial PET images. A similar VOI was used to obtain the SUVmax of the blood pool at the aortic arch from transaxial PET images, paying attention to not involve the vessel's walls. These two values were used to calculate a ratio with K (KL and KBP, respectively). Again, in the case of subjects with multiple PET/CT scans, dK, dKL and dKBP were calculated as the difference between the value at the second imaging evaluation and the value at the first scan.

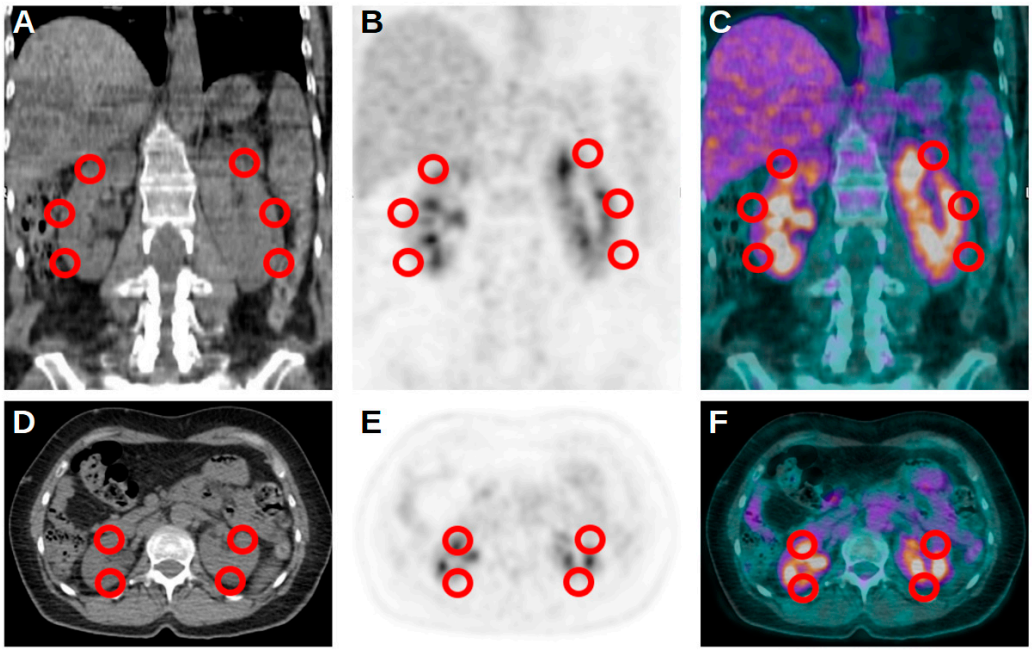

Figure 1. Representative and schematic figures in coronal (**A**–**C**) and axial (**D**–**F**) projection of the 5 VOIs used for the assessment of kidney uptake at [^{18}F]FDG PET/CT.

2.3. Statistical Analysis

Statistical analyses were performed using SPSS Software version 29.0.1.0 for Macintosh (New York, NY, USA). The descriptive analysis of categorical variables was carried out comprising the calculation of simple and relative frequencies. Numeric variables were described as mean, SD, minimum and maximum values (range).

Firstly, intraclass correlation coefficient (ICC) was used to calculate concordance and to evaluate the reproducibility of the assessment of renal uptakes at PET/CT between the two readers. To assess the correlation between Cr levels and PET/CT parameters, Pearson's test was applied. The same analysis was also performed to search for a correlation between eGFR levels and PET/CT parameters. Similarly, the search for the presence of a possible correlation between dCr and dEGFR with PET/CT uptakes, the same statistic test was applied. The aforementioned analyses were performed considering all the cohort of the study, only patients without a kidney transplantation, the group of transplanted patients and also considering cut-off values of 1.2 mg/dL for Cr (the upper limit of normal Cr value in our institution) and of 60 mL/min/1.73 m^2 for the EGFR. For all the aforementioned statistics, a p-value < 0.05 was considered significant.

Renal PET/CT semiquantitative parameters were also compared between patients, dividing them on the basis of the aforementioned values of 1.2 mg/dL for Cr and 60 mL/min/1.73 m^2 for the EGFR. These analyses were performed using T-test and were applied to the total cohort of patients and to the group of patients without kidney transplantation. No analyses were taken into account for transplanted subjects, since most of them had Cr > 1.2 mg/dL and/or EGFR > 60 mL/min/1.73 m^2. Moreover, ANOVA test was used to search for significant differences in terms of renal uptakes at PET/CT between the different classes of renal impairment based on the EGFR. T-test and Chi-square test were used to compare blood glucose levels and the use of insulin replacement therapy between the different classes of patients included in the study. Again, a p-value < 0.05 was considered significant for all these statistics.

3. Results

A total of 339 patients were included in our study (190 male, 56%). The mean age was 65, standard deviation (SD) 14 and range 18–92 years. Some patients underwent more than a single [^{18}F]FDG PET/CT study and therefore the total number of scans included in

this study were 385. Most of the subjects had 2 functioning kidneys (303, 89.4%), 17 (5.0%) patients were functional monokidney, while 19 (5.6%) had a kidney transplantation. In particular, 17 subjects (5.0%) had renal tracer uptake only on the transplanted kidney, while 2 (0.6%) had uptake on both native and transplanted kidneys (Table 1).

Table 1. Characteristics of the 339 patients included in the study.

Characteristics	Number (%)
Age (mean ± SD, range)	65 ± 14, 18–92
Gender	
Male	190 (56.0%)
Female	149 (44.0%)
Kidneys Status	
Functional monokidney	17 (5.0%)
Two functioning kidneys	303 (89.4%)
Transplanted	19 (5.6%)
Only transplanted kidney uptake	17 (5.0%)
Uptake on transplanted and native kidneys	2 (0.6%)
Cr (mg/dL) (mean ± SD, range)	2.1 ± 2.35, 0.36–11.1
Cr at the time of PET/CT	
<1.2 mg/dL	231 (60.0%)
≥1.2 mg/dL	154 (40.0%)
EGFR (mL/min/1.73m2) (mean ± SD, range)	63.8 ± 38.5, 4.2–139.7
EGFR at the time of PET/CT	
≥60 mL/min/1.73 m^2	226 (58.7%)
<60 mL/min/1.73 m^2	159 (41.3%)
CKD stage	
1	133 (39.2%)
2	85 (25.1%)
3	33 (9.7%)
4	27 (8.0%)
5	61 (18.0%)

SD: standard deviation; Cr: creatinine; EGFR: estimated glomerular filtration rate; PET/CT: positron emission tomography/computed tomography; CKD: chronic kidney disease.

The mean Cr value of our cohort was 2.1 (SD 2.35, range 0.36–11.1) and at the moment of the PET/CT scans, 231 patients (60.0%) had a Cr < 1.2 mg/dL, while the remaining 154 (40.0%) subjects had a Cr ≥ 1.2 mg/dL. In terms of the EGFR, the mean value of all the cohort was 63.8 (SD 38.5, range 4.2–139.7), with 226 (58.7%) subjects with a value ≥ 60 mL/min/1.73 m^2 at the time of PET/CT and the remaining 159 (41.3%) patients with an EGFR < 60 mL/min/1.73 m^2.

After classifying the patients based on CKD stage, 133 (39.2%) of them had a stage I disease, 85 (25.1%) had a stage II disease, 33 (9.7%) had a stage III disease, 27 (8.0%) had a stage IV disease and, lastly, 61 (18.0%) subjects had a stage V disease.

Blood glucose levels were collected at the moment of the PET/CT scan; the mean value was 113 mg/dL, range was 73–147 and SD was 21. No significant differences were reported for this parameter between patients with CKD and the controls (p-value 0.079), between subjects with a Cr value below and above 1.2 mg/dL (p-value 0.077) and between subjects with an EGFR below and above 60 mL/min/1.73 m^2 (p-value 0.098). Furthermore, at the moment of the PET/CT scan, 133 patients were using insulin replacement therapy; no significant differences in terms of the use of this therapy were underlined between patients with CKD and the controls (p-value 0.773), between subjects with a Cr value below and above 1.2 mg/dL (p-value 0.913) and between subjects with an EGFR below and above 60 mL/min/1.73 m^2 (p-value 0.676).

A strong concordance in the assessment of renal uptakes between the two readers was revealed by ICC analysis (r 0.848, p-value < 0.001). In the total cohort of the patients included in this study, we reported significant negative correlations for Cr values with K, KL and KBP. Significant positive correlations were instead underlined for the EGFR with K,

KL and KBP. Significant negative correlations were also demonstrated for dCr and dEGFR with dK, dKL and dKBP. When focusing only on the group of subjects without kidney transplantation, the same insights were confirmed and, again, Cr, dCr and dEGFR revealed a significant negative correlation with the PET/CT semiquantitative parameters, while the EGFR confirmed its positive correlation with K, KL and KBP. Moreover, when considering only transplanted patients, no significant correlations were underlined between the renal function parameters and PET/CT results. Similarly, no significant correlations between these data were reported in the group of subjects with a Cr < 1.2 mg/dL at the time of PET/CT. In contrast, when performing these analyses for subjects with a Cr $\geq$ 1.2 mg/dL at the time of PET/CT, negative significant correlations for Cr with K, KL and KBP, for dCr with dK, dKL and dKBP and for dEGFR with dK, dKL and dKBP were confirmed. Significant positive correlations were confirmed for the EGFR and PET/CT semiquantitative parameters. These findings on the presence of significant negative correlations for Cr, dCR and dEGFR and on the presence of a positive correlation for the EGFR with the PET/CT semiquantitative parameters were also confirmed when dividing the patients on the basis of an EGFR value of 60 mL/min/1.73 m^2 (Table 2; Figure 2).

Table 2. Correlation between renal functional parameters and PET/CT parameters.

	***p*-Value**	**Rho**
All patients (*n* = 339)		
Cr-K	<0.001	−0.33
Cr-KL	<0.001	−0.34
Cr-KBP	<0.001	−0.38
EGFR-K	<0.001	0.32
EGFR-KL	<0.001	0.35
EGFR-KBP	<0.001	0.42
dCr-dK	<0.001	−0.50
dCr-dKL	0.005	−0.41
dCr-dKBP	0.005	−0.42
dEGFR-dK	<0.001	−0.54
dEGFR-dKL	<0.001	−0.61
dEGFR-dKBP	<0.001	−0.59
Non-transplanted patients (*n* = 320)		
Cr-K	<0.001	−0.33
Cr-KL	<0.001	−0.34
Cr-KBP	<0.001	−0.39
EGFR-K	<0.001	0.34
EGFR-KL	<0.001	0.38
EGFR-KBP	<0.001	0.45
dCr-dK	<0.001	−0.53
dCr-dKL	0.005	−0.46
dCr-dKBP	<0.001	−0.54
dEGFR-dK	<0.001	−0.56
dEGFR-dKL	<0.001	−0.65
dEGFR-dKBP	<0.001	−0.72
Transplanted patients (*n* = 19)		
Cr-K	0.095	−0.32
Cr-KL	0.111	−0.31
Cr-KBP	0.114	−0.31
EGFR-K	0.867	−0.03
EGFR-KL	0.863	0.03
EGFR-KBP	0.562	0.12
dCr-dK	0.528	−0.26
dCr-dKL	0.926	0.04
dCr-dKBP	0.944	−0.03
dEGFR-dK	0.211	−0.49
dEGFR-dKL	0.391	−0.35
dEGFR-dKBP	0.541	−0.25

Table 2. *Cont.*

	***p*-Value**	**Rho**
Cr < 1.2 mg/dL (*n* = 231)		
Cr-K	0.199	−0.80
Cr-KL	0.119	−0.10
Cr-KBP	0.110	−0.10
EGFR-K	0.635	0.03
EGFR-KL	0.234	0.06
EGFR-KBP	0.128	0.10
dCr-dK	0.793	0.16
dCr-dKL	0.663	−0.26
dCr-dKBP	0.879	0.09
dEGFR-dK	0.638	0.28
dEGFR-dKL	0.981	−0.01
dEGFR-dKBP	0.731	−0.21
Cr ≥ 1.2 mg/dL (*n* = 154)		
Cr-K	<0.001	−0.46
Cr-KL	<0.001	−0.49
Cr-KBP	<0.001	−0.47
EGFR-K	<0.001	0.56
EGFR-KL	<0.001	0.54
EGFR-KBP	<0.001	0.56
dCr-dK	<0.001	−0.55
dCr-dKL	0.007	−0.43
dCr-dKBP	0.006	−0.44
dEGFR-dK	<0.001	−0.59
dEGFR-dKL	<0.001	−0.64
dEGFR-dKBP	<0.001	−0.60
EGFR ≥ 60(mL/min/1.73 m^2) (*n* = 226)		
Cr-K	<0.001	−0.33
Cr-KL	<0.001	−0.34
Cr-KBP	<0.001	−0.38
EGFR-K	<0.001	0.32
EGFR-KL	<0.001	0.46
EGFR-KBP	<0.001	0.42
dCr-dK	<0.001	−0.50
dCr-dKL	0.005	−0.41
dCr-dKBP	0.005	−0.42
dEGFR-dK	<0.001	−0.54
dEGFR-dKL	<0.001	−0.61
dEGFR-dKBP	<0.001	−0.59
EGFR < 60(mL/min/1.73 m^2)(*n* = 159)		
Cr-K	<0.001	−0.44
Cr-KL	<0.001	−0.49
Cr-KBP	<0.001	−0.46
EGFR-K	<0.001	0.51
EGFR-KL	<0.001	0.53
EGFR-KBP	<0.001	0.56
dCr-dK	<0.001	−0.55
dCr-dKL	0.007	−0.42
dCr-dKBP	0.006	−0.44
dEGFR-dK	<0.001	−0.59
dEGFR-dKL	<0.001	−0.64
dEGFR-dKBP	<0.001	−0.60

Cr: creatinine; K: kidney uptake; KL: kidney to liver ratio; KBP: kidney to blood pool ratio; EGFR: estimated glomerular filtration rate; dCr: differential Cr value; dK: differential kidney uptake; dKL: differential kidney to liver ratio; dKBP: differential kidney to blood pool ratio; dEGFR: differential estimated glomerular filtration rate; *n* = number.

Statistically significant differences in K, KL and KBP values were reported in all the cohort of our study, when dividing the patients based on a Cr value of 1.2 mg/dL. These find-

ings were confirmed when dividing them based on an EGFR value of 60 mL/min/1.73 m^2. Again, the same analysis performed in the cohort of transplanted patients confirmed the aforementioned findings. No analyses were performed in the group of subjects with a transplanted kidney, since it was a limited sample and most of them had Cr ≥ 1.2 mg/dL and/or EGFR > 60 mL/min/1.73 m^2. Lastly, statistically significant differences in terms of K, KL and KBP were underlined between the different classes of EGFR impairment (Table 3).

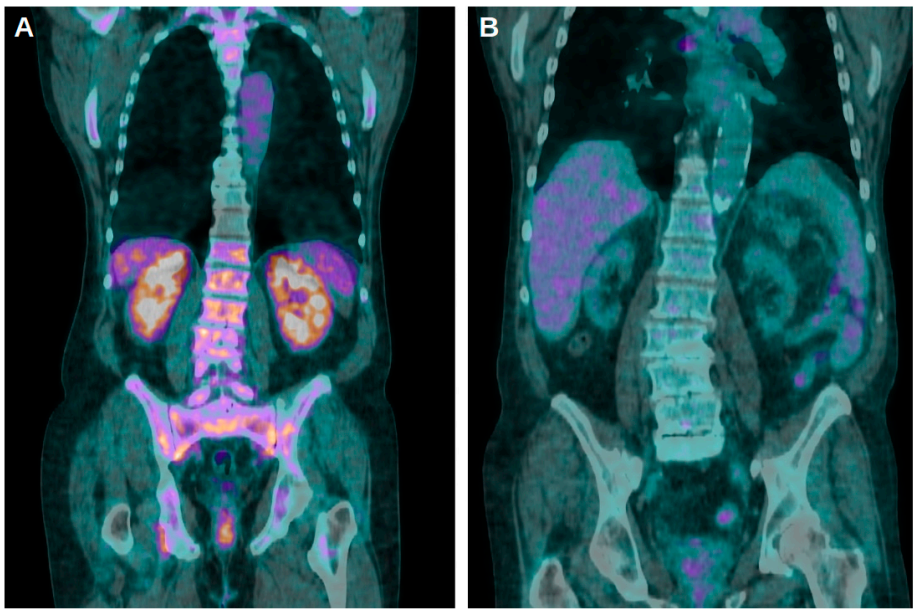

Figure 2. (**A**) Coronal fused [^{18}F]FDG PET/CT images of a patient with a Cr value of 1.41 mg/dL and an EGFR of 56.9 mL/min/1.73 m^2 at the moment of the scan. Stage of CKD was 3 and K, KL and KBP values were 8.85, 1.97 and 3.69, respectively. (**B**) Four years later, the same subjects again underwent a PET/CT scan: Cr raised to 9.12 mg/dL, EGFR dropped to 5.80 mL/min/1.73 m^2 and the stage of CKD was 5. K, KL and KBP were 1.82, 0.79 and 1.01, respectively.

Table 3. Correlation between class of renal impairment, creatinine and EGFR with PET/CT parameters.

	K	*p*-Value	KL	*p*-Value	KBP	*p*-Value
All patients (*n* = 339)						
Cr		<0.001		<0.001		<0.001
<1.2 mg/dL (*n* = 231)	4.63		1.78		2.36	
≥1.2 mg/dL (*n* = 154)	3.35		1.13		1.44	
EGFR		<0.001		<0.001		<0.001
≥60 (mL/min/1.73 m^2) (*n* = 226)	4.66		1.79		2.38	
<60 (mL/min/1.73 m^2) (*n* = 159)	3.33		1.14		1.44	
Non-transplanted patients (*n* = 320)						
Cr		<0.001		<0.001		<0.001
<1.2 mg/dL (*n* = 231)	4.66		1.79		2.37	
≥1.2 mg/dL (*n* = 154)	3.16		1.03		1.32	
EGFR		<0.001		<0.001		<0.001
≥60 (mL/min/1.73 m^2) (*n* = 226)	4.69		1.79		2.39	
<60 (mL/min/1.73 m^2) (*n* = 159)	3.15		1.04		1.32	
EGFR (*n* = 339)		<0.001		<0.001		<0.001
≥90 (mL/min/1.73 m^2) (*n* = 133)	4.76		1.85		2.49	
60–89 (mL/min/1.73 m^2) (*n* = 85)	4.51		1.68		2.21	
30–59 (mL/min/1.73 m^2) (*n* = 33)	4.36		1.46		1.90	
15–29 (mL/min/1.73 m^2) (*n* = 27)	3.14		1.16		1.41	
<15 (mL/min/1.73 m^2) (*n* = 61))	2.69		0.91		1.14	

Cr: creatinine; K: kidney uptake; KL: kidney to liver ratio; KBP: kidney to blood pool ratio; EGFR: estimated glomerular filtration rate; *n* = number.

4. Discussion

It is known that kidney function is one of the main determinants of [^{18}F]FDG excretion and, as mentioned before, different studies have tried to investigate a possible influence of renal failure on the interpretation of PET/CT imaging and on renal uptake with heterogeneous results [8,23,27].

Our findings revealed statistically significant K, KL and KBP values between different classes of renal impairment, between groups with different Cr values and between different EGFR values for the total cohort of patients and in the case of subjects without kidney transplantation. These analyses could not be performed for transplanted patients since most of them had a significant impairment of renal function. Moreover, statistically significant negative correlations between Cr values and renal [^{18}F]FDG uptake in the total cohort of patients included in this study and in most of the subgroups evaluated during the analyses were reported. Similarly, in most of the cases, statistically significant positive correlations between the EGFR and renal uptakes were reported. A possible explanation for these findings is the fact that an impairment of renal function, related to an increase in Cr values, could determine a reduction in glucose metabolic activity in the kidneys and therefore a reduction in tracer uptake. Interestingly, these insights were also confirmed when analyzing the temporal evolution of Cr blood levels and the evolution of renal uptakes in the case of patients with multiple PET/CT scans. In contrast, a significant negative correlation was reported between dEGFR and the evolution of renal PET uptakes; however, in order to interpret this different finding compared to the aforementioned positive correlation of the EGFR, it is important to consider that only a small sample of patients were studied with more than a single PET/CT scan.

No significant correlations were reported in the group of patients that had a kidney transplantation and in the group of subjects with a Cr value < 1.2 mg/dL. The first finding is in concordance with the findings reported by Jadoul et al. [28], who revealed that the uptake of [^{18}F]FDG by renal allografts is not significantly impacted by CKD. The fact that no significant correlations were underlined for patients with a blood Cr value < 1.2 mg/dL is an insight that could be taken into account in the day life interpretation of [^{18}F]FDG PET/CT scans, since the possible presence of reduced renal uptake could reflect the presence of an unknown impairment of the renal function of the patient. It is worth underlining that we reported a significant correlation between kidney uptakes and the EGFR in the group of patients that had a value $\geq$ 60 mL/min/1.73 m^2; however, this insight was not confirmed in the group of subjects that had a Cr value < 1.2 mg/dL. By definition, these two subgroups should contain most of the same patients as a low Cr and high EGFR are correlated and since the formula used to calculate the EGFR includes Cr. A possible explanation for this interesting finding could be the fact that according to the CKD-EPI formula, the calculation of the EGFR should include other parameters, such as sex and age, resulting therefore in some differences between Cr and EGFR values. In fact, Cr only expresses a serum marker and is not used to classify the degree of renal functional impairment; instead, this partition is based on the EGFR, which represents the estimated function of the kidney and is therefore a more reliable tool.

As previously mentioned, kidneys are organs that can excrete [^{18}F]FDG through the urinary tract; therefore, the assessment of renal tracer uptake could be impaired by the presence of radioactive urine in the renal pelvis [27,29]. Our findings, however, revealed a strong concordance in the assessment of renal parenchymal uptakes between the two readers, a finding that is in concordance with what was previously underlined by Jadoul et al. [30] when assessing the repeatability and reproducibility of the quantification of [^{18}F]FDG uptake by kidney allograft. As mentioned, it has also been reported that kidney [^{18}F]FDG uptake is related to the degree of sensitivity to insulin and that renal failure indirectly impairs this sensitivity and therefore glucose metabolism [9,10]. We considered this phenomenon in our study and no significant differences in terms of blood glucose levels at the moment of the PET/CT scan or the use of insulin replacement therapy were reported between the different groups of subjects, therefore strengthening our findings.

Our work is not without limitations; first of all, its retrospective design. Furthermore, the problem of the quantification of renal uptake, which could be influenced by the presence of radioactive urine, has been described in the discussion, even if our data underlined a good concordance between the two readers. Moreover, some analyses have been performed in a restricted group of patients; therefore, wider samples should be used to confirm our findings.

5. Conclusions

In conclusion, a strong correlation for renal [^{18}F]FDG uptake with the Cr levels and EGFR was reported, with exceptions for the group of patients with a Cr value < 1.2 mg/dL and for the group with a kidney transplantation. High agreement between the two readers in the assessment of renal tracer uptakes was underlined.

Author Contributions: Conceptualization, F.D. and A.T.; methodology, F.D. and M.G.; writing—original draft preparation, F.D., M.G., A.R.P. and A.T.; writing—review and editing, F.D., A.R.P., M.G., N.M.L., A.T., D.A., D.R., N.M., G.R. and F.B. All authors have read and agreed to the published version of the manuscript.

Funding: This research received no external funding.

Institutional Review Board Statement: Ethical review and approval were waived for this study due to its retrospective de-sign, according to local laws and to the ethics committees of our center.

Informed Consent Statement: Informed consent was obtained from all subjects involved in the study.

Data Availability Statement: Data available on request due to privacy/ethical restrictions.

Conflicts of Interest: The authors declare no conflicts of interest.

References

1. Ammirati, A.L. Chronic Kidney Disease. *Rev. Assoc. Med. Bras.* **2020**, *66* (Suppl. S1), s03–s09. [CrossRef]
2. Charles, C.; Ferris, A.H. Chronic Kidney Disease. *Prim. Care* **2020**, *47*, 585–595. [CrossRef]
3. Inker, L.A.; Titan, S. Measurement and Estimation of GFR for Use in Clinical Practice: Core Curriculum 2021. *Am. J. Kidney Dis.* **2021**, *78*, 736–749. [CrossRef]
4. Kidney Disease: Improving Global Outcomes (KDIGO) Diabetes Work Group. KDIGO 2020 Clinical Practice Guideline for Diabetes Management in Chronic Kidney Disease. *Kidney Int.* **2020**, *98*, S1–S115. [CrossRef]
5. Casali, M.; Lauri, C.; Altini, C.; Bertagna, F.; Cassarino, G.; Cistaro, A.; Erba, A.P.; Ferrari, C.; Mainolfi, C.G.; Palucci, A.; et al. State of the art of 18F-FDG PET/CT application in inflammation and infection: A guide for image acquisition and interpretation. *Clin. Transl. Imaging* **2021**, *9*, 299–339. [CrossRef]
6. Altini, C.; Lavelli, V.; Ruta, R.; Ferrari, C.; Nappi, A.G.; Pisani, A.; Sardaro, A.; Rubini, G. Typical and atypical PET/CT findings in non-cancerous conditions. *Hell. J. Nucl. Med.* **2020**, *23*, 48–59. [CrossRef]
7. Dondi, F.; Albano, D.; Bellini, P.; Volpi, G.; Giubbini, R.; Bertagna, F. 18F-fluorodeoxyglucose PET and PET/computed tomography for the evaluation of immunoglobulin G4-related disease: A systematic review. *Nucl. Med. Commun.* **2022**, *43*, 638–645. [CrossRef]
8. Moran, J.K.; Lee, H.B.; Blaufox, M.D. Optimization of urinary FDG excretion during PET imaging. *J. Nucl. Med.* **1999**, *40*, 1352–1357.
9. Rebelos, E.; Mari, A.; Oikonen, V.; Iida, H.; Nuutila, P.; Ferrannini, E. Evaluation of renal glucose uptake with [18F]FDG-PET: Methodological advancements and metabolic outcomes. *Metabolism* **2023**, *141*, 155382. [CrossRef]
10. Laffon, E.; Cazeau, A.L.; Monet, A.; de Clermont, H.; Fernandez, P.; Marthan, R.; Ducassou, D. The effect of renal failure on 18F-FDG uptake: A theoretic assessment. *J. Nucl. Med. Technol.* **2008**, *36*, 200–202. [CrossRef]
11. Reuter, S.; Schnöckel, U.; Edemir, B.; Schröter, R.; Kentrup, D.; Pavenstädt, H.; Schober, O.; Schlatter, E.; Gabriëls, G.; Schäfers, M. Potential of noninvasive serial assessment of acute renal allograft rejection by 18F-FDG PET to monitor treatment efficiency. *J. Nucl. Med.* **2010**, *51*, 1644–1652. [CrossRef] [PubMed]
12. Kidera, E.; Koyasu, S.; Hayakawa, N.; Ishimori, T.; Nakamoto, Y. Association between diffuse renal uptake of 18F-FDG and acute kidney injury. *Ann. Nucl. Med.* **2022**, *36*, 351–359. [CrossRef] [PubMed]
13. Lovinfosse, P.; Weekers, L.; Bonvoisin, C.; Bovy, C.; Grosch, S.; Krzesinski, J.M.; Hustinx, R.; Jouret, F. Fluorodeoxyglucose F(18) Positron Emission Tomography Coupled With Computed Tomography in Suspected Acute Renal Allograft Rejection. *Am. J. Transplant.* **2016**, *6*, 310–316. [CrossRef]
14. Hanssen, O.; Weekers, L.; Lovinfosse, P.; Jadoul, A.; Bonvoisin, C.; Bouquegneau, A.; Grosch, S.; Huynen, A.; Anglicheau, D.; Hustinx, R.; et al. Diagnostic yield of 18 F-FDG PET/CT imaging and urinary CXCL9/creatinine levels in kidney allograft subclinical rejection. *Am. J. Transplant.* **2020**, *20*, 1402–1409. [CrossRef] [PubMed]

15. Geist, B.K.; Baltzer, P.; Fueger, B.; Hamboeck, M.; Nakuz, T.; Papp, L.; Rasul, S.; Sundar, L.K.S.; Hacker, M.; Staudenherz, A. Assessing the kidney function parameters glomerular filtration rate and effective renal plasma flow with dynamic FDG-PET/MRI in healthy subjects. *EJNMMI Res.* **2018**, *8*, 37. [CrossRef] [PubMed]
16. Fink, J.C.; Lodge, M.A.; Smith, M.F.; Hinduja, A.; Brown, J.; Dinits-Pensy, M.Y.; Dilsizian, V. Pre-clinical myocardial metabolic alterations in chronic kidney disease. *Cardiology* **2010**, *116*, 160–167. [CrossRef] [PubMed]
17. Bural, G.G.; Torigian, D.A.; Sözmen, M.; Houseni, M.; Alavi, A. Comparison of atherosclerotic inflammation and calcification in subjects with end stage renal disease (ESRD) on hemodialysis to normal controls utilizing 18F-FDG PET/CT. *Hell. J. Nucl. Med.* **2018**, *21*, 169–174. [CrossRef] [PubMed]
18. Yoon, H.E.; Kim, Y.; Kim, S.D.; Oh, J.K.; Chung, Y.A.; Shin, S.J.; Yang, C.W.; Seo, S.M. A Pilot Trial to Examine the Changes in Carotid Arterial Inflammation in Renal Transplant Recipients as Assessed by 18F-Fluorodeoxyglucose (18F-FDG) Positron Emission Tomography Computed Tomography (PET/CT). *Ann. Transplant.* **2018**, *23*, 412–421. [CrossRef]
19. Lawal, I.O.; Popoola, G.O.; Lengana, T.; Ankrah, A.O.; Ebenhan, T.; Sathekge, M.M. Diagnostic utility of 18F-FDG PET/CT in fever of unknown origin among patients with end-stage renal disease treated with renal replacement therapy. *Hell. J. Nucl. Med.* **2019**, *22*, 70–75. [CrossRef]
20. Tek Chand, K.; Chennu, K.K.; Amancharla Yadagiri, L.; Manthri Gupta, R.; Rapur, R.; Vishnubotla, S.K. Utility of 18 F-FDG PET/CT scan to diagnose the etiology of fever of unknown origin in patients on dialysis. *Hemodial. Int.* **2017**, *21*, 224–231. [CrossRef]
21. Tseng, J.R.; Lin, C.W.; Chen, S.H.; Yen, T.H.; Lin, P.Y.; Lee, M.H.; Yen, T.C. Clinical Usefulness of ^{18}F-FDG PET/CT for the Detection of Infections of Unknown Origin in Patients Undergoing Maintenance Hemodialysis. *J. Nucl. Med.* **2015**, *56*, 681–687. [CrossRef] [PubMed]
22. Pijl, J.P.; Glaudemans, A.W.J.M.; Slart, R.H.J.A.; Kwee, T.C. 18F-FDG PET/CT in Autosomal Dominant Polycystic Kidney Disease Patients with Suspected Cyst Infection. *J. Nucl. Med.* **2018**, *59*, 1734–1741. [CrossRef] [PubMed]
23. Akers, S.R.; Werner, T.J.; Rubello, D.; Alavi, A.; Cheng, G. 18F-FDG uptake and clearance in patients with compromised renal function. *Nucl. Med. Commun.* **2016**, *37*, 825–832. [CrossRef] [PubMed]
24. Otomi, Y.; Arai, Y.; Otomo, M.; Irahara, S.; Terazawa, K.; Kubo, M.; Abe, T.; Shinya, T.; Otsuka, H.; Harada, M. Increased physiological [18F]FDG uptake in the liver and blood pool among patients with impaired renal function. *Nucl. Med. Rev. Cent. East. Eur.* **2022**, *25*, 95–100. [CrossRef] [PubMed]
25. Toriihara, A.; Kitazume, Y.; Nishida, H.; Kubota, K.; Nakadate, M.; Tateishi, U. Comparison of FDG-PET/CT images between chronic renal failure patients on hemodialysis and controls. *Am. J. Nucl. Med. Mol. Imaging* **2015**, *5*, 204–211. [PubMed]
26. Kode, V.; Karsch, H.; Osman, M.M.; Muzaffar, R. Impact of Renal Failure on F18-FDG PET/CT Scans. *Front. Oncol.* **2017**, *21*, 155. [CrossRef] [PubMed]
27. Qiao, H.; Bai, J.; Chen, Y.; Tian, J. Kidney modelling for FDG excretion with PET. *Int. J. Biomed. Imaging* **2007**, *2007*, 63234. [CrossRef] [PubMed]
28. Jadoul, A.; Lovinfosse, P.; Weekers, L.; Delanaye, P.; Krzesinski, J.M.; Hustinx, R.; Jouret, F. The Uptake of 18F-FDG by Renal Allograft in Kidney Transplant Recipients Is Not Influenced by Renal Function. *Clin. Nucl. Med.* **2016**, *41*, 683–687. [CrossRef]
29. Engel, H.; Steinert, H.; Buck, A.; Berthold, T.; Huch Böni, R.A.; von Schulthess, G.K. Whole-body PET: Physiological and artifactual fluorodeoxyglucose accumulations. *J. Nucl. Med.* **1996**, *37*, 441–446.
30. Jadoul, A.; Lovinfosse, P.; Bouquegneau, A.; Weekers, L.; Pottel, H.; Hustinx, R.; Jouret, F. Observer variability in the assessment of renal 18F-FDG uptake in kidney transplant recipients. *Sci. Rep.* **2020**, *10*, 4617. [CrossRef]

Disclaimer/Publisher's Note: The statements, opinions and data contained in all publications are solely those of the individual author(s) and contributor(s) and not of MDPI and/or the editor(s). MDPI and/or the editor(s) disclaim responsibility for any injury to people or property resulting from any ideas, methods, instructions or products referred to in the content.

Check for updates

Hematological Oncology

WILEY

ORIGINAL ARTICLE OPEN ACCESS

Prognostic Role of Pretreatment Tumor Burden and Dissemination Features From 2-[^{18}F]FDG PET/CT in Advanced Mantle Cell Lymphoma

Domenico Albano[1,2] | Nicola Bianchetti[3] | Anna Talin[2] | Francesco Dondi[1,2] | Alessandro Re[3] | Alessandra Tucci[3] | Francesco Bertagna[1,2]

[1]Nuclear Medicine Department, ASST Spedali Civili Brescia, Brescia, Italy | [2]Università degli Studi di Brescia, Brescia, Italy | [3]Division of Hematology, ASST Spedali Civili, Brescia, Italy

Correspondence: Domenico Albano (doalba87@libero.it; domenico.albano@unibs.it)

Received: 11 June 2024 | **Revised:** 4 November 2024 | **Accepted:** 16 November 2024

Funding: The authors received no specific funding for this work.

Keywords: 18F-FDG PET/CT | dissemination | Dmax | Mantle cell lymphoma | MTV | prognosis

ABSTRACT

Mantle cell lymphoma (MCL) is an aggressive non-Hodgkin lymphoma with poor prognosis. The usefulness of fluorine-18-fluorodeoxyglucose positron emission tomography/computed tomography (2-[^{18}F]FDG PET/CT) and its parameters in the evaluation of treatment response and prognosis is not yet clear. The aim of this study was to investigate the prognostic role of tumor burden and tumor dissemination features derived by 2-[^{18}F]FDG PET/CT in advanced MCL. We retrospectively included 120 patients with advanced MCL who underwent baseline 2- 2-[^{18}F]FDG PET/CT and end-of-treatment (eot) PET/CT. The baseline-PET images were analyzed visually and semi-quantitatively by measuring the maximum standardized uptake value body weight (SUVbw), lean body mass (SUVlbm), body surface area (SUVbsa), metabolic tumor volume (MTV), total lesion glycolysis (TLG) and dissemination features (Dmax and Dmax-bsa). EotPET/CT was judged according to the Lugano classification. Progression-free survival (PFS) and overall survival (OS) were plotted according to the Kaplan–Meier method. At a median follow-up of 59 months, relapse/progression occurred in 68 patients while death in 38 patients with a median PFS and OS of 27.2 and 57.6 months, respectively. MIPI score, Bulky disease, Ki-67 index, metabolic response, pretreatment MTV and TLG were significantly associated with PFS at univariate analysis, but only metabolic response, MTV and TLG were confirmed to be independent prognostic factors. Considering OS, only dissemination features were demonstrated to be prognostic features. In conclusions, metabolic response and metabolic tumor burden parameters (MTV and TLG) are strongest predictor of PFS, while dissemination features may have a significant role for predicting OS.

1 | Introduction

Mantle cell lymphoma (MCL) is a rare subtype of aggressive B cell non-Hodgkin's lymphoma (NHL) representing about 3%–10% of all NHLs in Western countries [1]. The median age of diagnosis is between 60 and 70 years, while clinical presentations are quite various (ranging from asymptomatic indolent clinical course to symptomatic appearance). The pathogenesis of MCL is very complex including several molecular aberrations, environmental risk factors, and/or familiar risk [2]. MCL usually has a high risk of relapse and poor prognosis despite recent improvements in the treatment field [3]. At the moment, several biological,

This is an open access article under the terms of the Creative Commons Attribution License, which permits use, distribution and reproduction in any medium, provided the original work is properly cited.

© 2024 The Author(s). *Hematological Oncology* published by John Wiley & Sons Ltd.

pathological, and imaging markers to stratify these patients are studied with controversial results. A specific prognostic index for MCL was created and called The Mantle Cell Lymphoma International Prognostic Index (MIPI) [4] and demonstrated to be a strong predictor of outcome. However, also other prognostic markers, such as blastoid variant, Ki-67 index higher than 30%, and TP53 mutation/deletion were tested with positive findings [5–7]. Preliminary evidence about a potential prognostic role of fluorine-18-fluorodeoxyglucose positron emission tomography/computed tomography (2-[^{18}F]FDG PET/CT) in MCL has been emerging, especially concerning metabolic tumor burden features and metabolic response after treatment applying Lugano criteria [8–10]. Lugano treatment response classification is a system based on the application of the Deauville five-point scale for reporting response by 2-[^{18}F]FDG PET/CT in HL and several NHL [11]. Recently, a new PET-derived metabolic variable describing the dissemination of the hypermetabolic disease in the body was studied in lymphomas: the maximum tumor dissemination (Dmax) [12]. Dmax was defined as the maximum distance between the two farthest lesions with increased uptake on 2-[^{18}F]FDG PET/CT. In MCL, only one research investigated the role of Dmax showing no prognostic usefulness of this feature [10]. A more sophisticated prognostic stratification model is desirable to identify subgroups who might benefit from more aggressive therapies, or in whom the prognosis is already sufficiently good to obviate more conservative treatment plans. For this reason, the idea to incorporate in this prognostic model also metabolic features may be of clinical interest. This study aimed to analyze whether 2-[^{18}F]FDG PET/CT and its parameters alone or combined with classical clinical and epidemiological variables may prognosticate outcome in MCL.

2 | Materials and Methods

2.1 | Patients Selection

This research was a monocentric retrospective study. Using our institutional Radiology Information System (RIS), we have screened all the patients studied with 2-[^{18}F]FDG PET/CT in our Nuclear Medicine center from February 2007 until January 2023. Inclusion criteria were (1) histological diagnosis of MCL, (2) presence of baseline and end-of-treatment (eot) 2-[^{18}F]FDG PET/CT, (3) intermediate-advanced stage disease (stage II, III, IV), (4) absence of concomitant malignancy, (4) presence of at least 12 months of follow-up. Applying these criteria (Figure 1), 120 patients were included in this research. For each patient, the main epidemiological (sex, age at diagnosis), clinical (MIPI score, Ann Arbor stage, MCL variant, presence of B symptoms, presence of bulky disease, LDH and β2-microglobulin level at diagnosis, Ki-67 level, kind of therapy) were collected. To define bulky disease, we considered any mass measuring at least 10 cm or more in diameter by any imaging study, or with a diameter equal or greater than one-third of the internal transverse diameter of the thorax. Proliferative activity, measured by Ki-67 score, was available in 106 patients; the Ki-67 expression level was divided into two groups: ≤ 30% and > 30% as suggested previously in the literature [6]. All patients were treated according to the institution's standard protocol with chemotherapy regimen. Fifty-eight patients according to R-CHOP (Rituximab, Cyclophosphamide, Hydroxydoxorubicine, Oncovin and Prednisone) or alternating R-CHOP/R-DHAP (Rituximab, Dexamethasone, high dose Ara-C cytarabine, Cisplatin) regimen followed by autologous stem cell transplantation; 46 patients were treated according to R-BAC regimen up to six cycles of immuno-chemotherapy including Rituximab, Bendamustine and Cytarabine; 4 patients received R-HyperCVAD and the remaining 12 patients were treated according to MCL 0208 trial which consisted of high-dose chemotherapy additional with Rituximab, followed by autologous stem cell transplantation and Lenalidomide as maintenance therapy. Globally 70 patients received autologous stem cell transplantation. Also elderly patients were treated because in fit status.

2.2 | 2-[^{18}F]FDG PET/CT Imaging and Analysis

Baseline 2-[^{18}F]FDG PET/CT was performed before any kind of treatment (chemotherapy and/or radiotherapy), eotPET/CT was performed after 6 cycles of chemotherapy or less in case of conditions that contraindicated further cycles. Median time from PET/CT and starting treatment was 7 days (range 1–14 days). No patients received a watch and wait approach.

2-[^{18}F]FDG PET/CT was performed after at least 4 h fasting and with glucose blood level less than 150 mg/dL. Sixty minutes after the injection by vein of an activity of 3.5–4.5 MBq/Kg of radiotracer, 2-[^{18}F]FDG PET/CT scans were acquired. Usually, the field of view was from the skull basis to the mid-thigh. Tomographs where scans were acquired: a Discovery 690 or a Discovery ST scanner (General Electric Healthcare, Milwaukee, WI, USA) with standard CT parameters (80 mA, 120 Kv, without contrast; 2.5–3.5 min per bed-PET-step of 15 cm); the reconstruction was performed in a 128 × 128 matrix and 60 cm field of view. Reconstruction protocol consists of ordered subset expectation maximization (OSEM), filter cut-off 5 mm, 21 subsets and 2 iterations for both scanners.

2-[^{18}F]FDG PET/CT scans for all patients were visually and semiquantitatively revised by an expert nuclear medicine physician (DA) who was blinded to the patient clinical data and outcome.

The PET images were analyzed from a qualitative and semiquantitative point of view. Concerning qualitative analysis, every focal uptake different from physiological distribution and background was considered suggestive of disease. Bone marrow disease was considered if there was a focal uptake; spleen disease was considered if there was focal uptake in the spleen or diffuse uptake higher than 1.5 of the liver background. EotPET were classified according to Lugano criteria applying Deauville Scores [11]. According to Deauville score 2-[^{18}F]FDG PET/CT was interpreted as follows: 1 = no uptake above background, 2 = uptake equal to or lower than mediastinum, 3 = uptake higher than mediastinum, and lower than liver, 4 = uptake moderately increased compared to the liver and 5 = uptake markedly increased compared to the liver. Concerning the Deauville scores, PET/CT scans were defined as a complete metabolic response in the presence of Deauville scores 1–3 and not complete metabolic response in the presence of Deauville scores 4–5. Concerning semiquantitative

10991069, 2025, 1, Downloaded from https://onlinelibrary.wiley.com/doi/10.1002/hon.70009 by Anna Talin - Cochraneltalia , Wiley Online Library on [29/11/2024]. See the Terms and Conditions (https://onlinelibrary.wiley.com/terms-and-conditions) on Wiley Online Library for rules of use; OA articles are governed by the applicable Creative Commons License

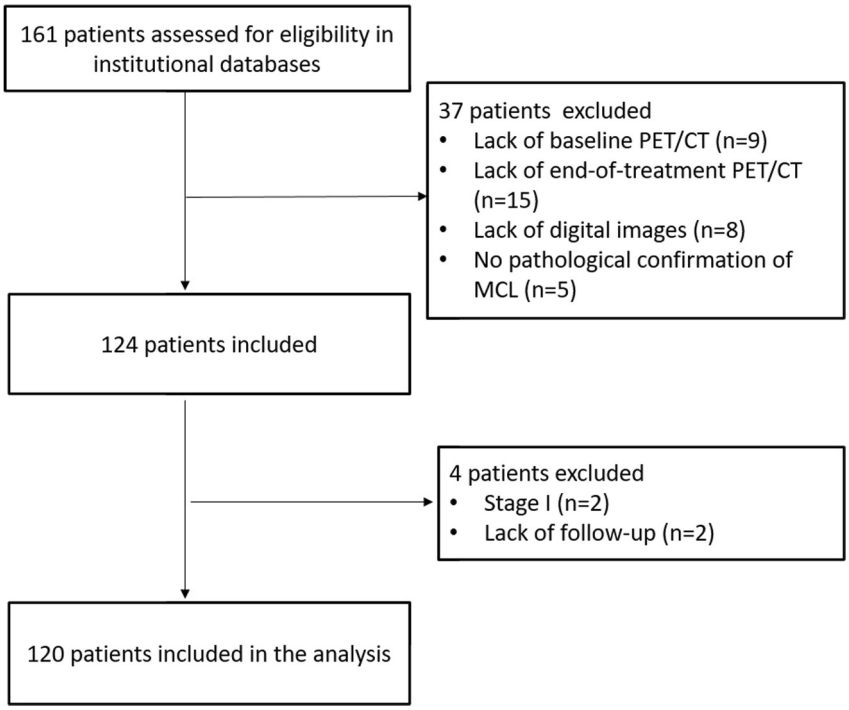

FIGURE 1 | Flow diagram of patients included in the study.

measurements, we measured the maximum standardized uptake value corrected for body weight (SUVbw), SUV corrected for body surface area (SUVbsa), SUV corrected for lean body mass (SUVlbm), metabolic tumor volume (MTV), total lesion glycolysis (TLG), Dmax and Dmax corrected for bsa. For these measurements, we used LIFEx software [13].

SUV values were measured in the lesion with the highest uptake by drawing a region of interest over the area of maximum activity and the SUVmax was calculated as the highest SUV of the pixels within the ROI. MTV was calculated using the 41% SUVmax threshold as suggested by the European Association of Nuclear Medicine [14]. TLG was subsequently calculated as the sum of MTV*SUVmean for each uptake. To calculate Dmax, the Euclidean formula measured the distance between all pairs of lesions (including both nodal and extranodal) recording the greatest lesion distance. For Dmax-bsa, we applied the Du Bois method [15].

2.3 | Statistical Analysis

The statistical analyses were performed with Statistical Package for Social Science (SPSS) version 24.0 for Windows (IBM, Chicago, Illinois, USA). The descriptive analysis of categorical variables included the simple and relative frequencies; the numeric variables as average, standard deviation, minimum and maximum.

Receiver operating characteristic (ROC) curve analyses were used to identify the best thresholds of metabolic parameters in the light of which interpret the results of progression free survival (PFS) and overall survival (OS) (Table S1). PFS was calculated from the date of baseline 2-[^{18}F]FDG PET/CT to the date of first relapse, disease progression, or the date of last follow-up. Progression/relapse was considered when a dimensional and/or numerical increase of lesion at CT or PET/CT was demonstrated. OS was calculated from the date of baseline 2-[^{18}F]FDG PET/CT to the date of death from any cause or to the date of last follow-up. Survival curves were plotted according to the Kaplan–Meier method and differences between groups were analyzed by using a two-tailed log-rank test. Cox regression was used to estimate the hazard ratio (HR) and its confidence interval (CI). A *p-value* of < 0.05 was considered statistically significant.

3 | Results

3.1 | Tumors Characteristics at Baseline

In our population, there was a prevalence of males ($n = 90$) and the average age was 65.6 years (range 30–89). Most patients were classified as advanced stage (stage IV) with 104 cases, followed by stage III with 11 cases and stage II with 5 cases. Bulky disease, splenomegaly and B symptoms were described in 16, 49 and 29 patients, respectively. MIPI score was low in 35 cases, intermediate in 45 and high in the remaining 39. Ki-67 index was low (< 30%) in most patients ($n = 68$). 2-[^{18}F]FDG PET/CT resulted all positive showing at least two hypermetabolic lesions. The mean SUVbw of the lesion with higher ^{18}F-FDG uptake at the baseline was 10.4 (range 3.5–14.5); mean SUVlbm 6.9 (range 2.5–9.5), mean SUVbsa 2.5 (range 0.7–6.8), mean MTV 491 cm^3 (2–4000 cm^3) mean TLG 3060 (6–23000), mean Dmax 54.6 cm (6–82) and mean Dmax-bsa 29.5 (3.3–49). All patients had ^{18}F-FDG-avid nodal disease; extranodal involvement included bone marrow in 34 (28%) patients and gastrointestinal system in 16 (13%). All the main features of the patients are summarized in Table 1.

10991069, 2025, 1, Downloaded from https://onlinelibrary.wiley.com/doi/10.1002/hon.70009 by Anna Talin - Cochraneltalia , Wiley Online Library on [29/11/2024]. See the Terms and Conditions (https://onlinelibrary.wiley.com/terms-and-conditions) on Wiley Online Library for rules of use; OA articles are governed by the applicable Creative Commons License

TABLE 1 | The main clinical characteristics of the entire population included (n = 120 patients).

	Patients n (%)	Average ± SD (range)	Median
Sex male	90 (75%)		
Sex female	30 (25%)		
Age (years)		65.6 ± 10 (30–89)	63
Tumor stage at diagnosis (Ann Arbor)			
I	0 (0%)		
II	5 (4%)		
III	11 (9%)		
IV	104 (87%)		
Blastoid variant	16 (13%)		
B symptoms	29 (24%)		
LDH			
Normal	77 (64%)		
Increased	43 (36%)		
β2 microglobulin			
Normal	82 (68%)		
Increased	38 (32%)		
Bulky disease	16 (13%)		
Splenomegaly	49 (41%)		
Ki-67 score[a]			
< 30%	68 (64%)		
≥ 30%	38 (36%)		
MIPI score			
Low	36 (30%)		
Intermediate	45 (37.5%)		
High	39 (32.5%)		
SUVbw		10.4 ± 6 (3.5–9.7)	9
SUVlbm		6.9 ± 4.1 (2.5–9.5)	6
SUVbsa		2.5–1.5 (0.7–6.8)	2.5
MTV		491 ± 696 (2–4000)	358
TLG		3060 ± 4625 (6–23000)	2950
Dmax		54.6 ± 19.5 (6–82)	48.8
Dmax-bsa		29.5 ± 11.1 (3.3–49)	25.9

Abbreviations: LDH, lactate dehydrogenase; MIPI, Mantle international prognostic index; MTV, metabolic tumor volume; SUVbsa, body surface area; SUVbw, standardized uptake value body weight; SUVlbm, lean body mass; TLG, total lesion glycolysis.
[a]Not available in 14 patients.

3.2 | Treatment Response Setting

Based on Lugano classification, complete metabolic response was registered in 83 (70%) patients, and not complete response in 35 (30%) patients. Two patients died before the execution of eotPET/CT. Among complete metabolic responses, Deauville scores 1,2,3 were defined in 62, 12 and 9 patients, respectively. Among not complete metabolic responses, Deauville scores 4 and 5 were present in 19 and 16 cases. Comparing complete and not complete response groups, only age and Ki-67 scores were significantly different (p = 0.011); particularly, age and Ki-67 index were significantly higher in patients that did not reach complete response. No significant difference was demonstrated comparing the metabolic PET features between not complete and complete response groups (Table 2).

3.3 | Role of 2-[^{18}F]FDG PET/CT in Predicting PFS

At a median follow-up of 59 months, relapse or progression of disease occurred in 68 patients with an average time of 26 months (range: 2–113 months) from the baseline PET/CT. Median PFS was 27.2 months. Three-year and 5-year PFS were 50% and 36%, respectively. At univariate analysis, the presence of bulky disease, Ki-67 level, MIPI score, metabolic response at

10991069, 2025, 1, Downloaded from https://onlinelibrary.wiley.com/doi/10.1002/hon.70009 by Anna Talin - Cochraneltalia , Wiley Online Library on [29/11/2024]. See the Terms and Conditions (https://onlinelibrary.wiley.com/terms-and-conditions) on Wiley Online Library for rules of use; OA articles are governed by the applicable Creative Commons License

TABLE 2 | Comparison of baseline metabolic PET/CT features between no response and complete/partial response groups at end-of-treatment.

	End of treatment response		
Parameter	**Complete metabolic response *n* 83**	**Not complete metabolic response *n* 35**	***p* value**
Gender M: F	61:22	29:8	0.680
Age, mean ± SD	64.1 ± 12	69 ± 13	0.011
Stage IV	71 (68%)	33 (94%)	0.553
Blastoid variant	9 (11%)	7 (20%)	0.578
B symptoms	20 (24%)	9 (26%)	0.685
LDH increased	25 (30%)	18 (51%)	0.787
β2 microglobulin increased	22 (27%)	16 (46%)	0.459
Bulky disease	11 (13%)	5 (14%)	0.882
Splenomegaly	35 (42%)	14 (40%)	0.828
Ki-67 score ≥ 30%	21 (25%)	17 (49%)	0.011
MIPI score intermediate/high	56 (67%)	28 (80%)	0.172
SUVbw, mean ± SD	8.7 ± 3.1	9.7 ± 4	0.320
SUVlbm, mean ± SD	6.5 ± 2.7	7.3 ± 2.8	0.347
SUVbsa, mean ± SD	2.2 ± 0.8	2.5 ± 0.9	0.195
MTV, mean ± SD	486 ± 99	530 ± 121	0.757
TLG, mean ± SD	2810 ± 1450	3831 ± 1345	0.283
Dmax, mean ± SD	55.5 ± 19.8	54 ± 21.2	0.718
Dmax bsa, mean ± SD	29.9 ± 10.1	29.4 ± 12	0.835

Abbreviations: bsa, body surface area; bw, body weight; F, female; lbm, lean body mass; M, male; MIPI, Mantle Cell Lymphoma International Prognostic Index; MTV, total metabolic tumor volume; SD, standard deviation; SUV, standardized uptake value; TLG, total lesion glycolysis.

eotPET/CT, MTV and TLG were significantly associated with PFS (Table 3). PFS was statistically significantly longer in patients with low-to-intermediate MIPI score, complete metabolic response at eotPET/CT DC, low MTV and low TLG (Figure 2). At multivariate analysis, eotPET/CT, MTV and TLG were confirmed to be independent prognostic factors ($p < 0.001$; $p = 0.003$; $p = 0.042$) (Table 4). Concerning PFS, dissemination features were not associated with the outcome. The combination of metabolic response and baseline MTV stratified better patients PFS (Figure 3). Patients with high MTV and incomplete response at eotPET/CT had the worse PFS. The median PFS of patients with low MTV and complete metabolic response was 58.9 months, of the patients with low MTV and incomplete metabolic response 48 months, of the patients with complete response and high MTV 29.7 months and of patients with incomplete metabolic response and high MTV 8 months.

3.4 | Role of 2-[^{18}F]FDG PET/CT in Predicting OS

Death occurred in 38 patients with an average time of 37 months (range 2–151). In most patients ($n = 27$) the death was considered directly related to the lymphoma or therapy; in the remaining 11 cases the causes of death are not related to the lymphoma. The median OS was 57.6 months. Three-year and 5-year OS were 78% and 65%, respectively. At univariate analysis, stage IV, Dmax and Dmax-bsa were significantly correlated with OS (Table 3). OS was statistically significantly longer in patients with low Dmax and low Dmax-bsa (Figure 4). At multivariate analysis, only Dmax bsa was confirmed to be an independent prognostic variable ($p = 0.025$) (Table 4). Concerning OS, all the other metabolic features showed to have no prognostic value.

4 | Discussion

MCL demonstrated to be a lymphoma variant with a high 2-[^{18}F]FDG PET/CT detection rate concerning nodal diseases, while the diagnostic performances of PET/CT in the detection of gastrointestinal involvement and bone marrow (BM) infiltration are less good [16]. This is the reason why it is suggested to perform BM biopsy and GI endoscopy in the staging phase to classify correctly these patients. Both BM and the gastrointestinal tract are hard settings to examine with ^{18}F-FDG, due to the presence of physiologic uptake of this radiopharmaceutical in several inflammatory/infectious and functional conditions.

On the other hand, in the restaging field, especially in the evaluation of treatment response, 2-[^{18}F]FDG PET/CT seems to be an accurate tool better than morphological examinations [16]. Another potential advantage of PET/CT is the possibility to give prognostic information to predict disease aggressiveness and consequently affect patient management.

The first result of this study was the validation of the prognostic role of metabolic response categories applying Deauville scores. Deauville scores is a scale using the liver and blood-pool activity as the references to classify the degree of uptake of residual disease after therapy and it has been recommended for reporting both interim and end-of-treatment PET for HL and several

10991069, 2025, 1, Downloaded from https://onlinelibrary.wiley.com/doi/10.1002/hon.70009 by Anna Talin - Cochraneltalia , Wiley Online Library on [29/11/2024]. See the Terms and Conditions (https://onlinelibrary.wiley.com/terms-and-conditions) on Wiley Online Library for rules of use; OA articles are governed by the applicable Creative Commons License

TABLE 3 | Univariate analyses for progression free survival and overall survival.

	PFS		OS	
	***p* value**	**HR (95% CI)**	***p* value**	**HR (95% CI)**
Sex	0.483	1.600 (0.586–3.001)	0.610	1.135 (0.705–1.825)
Age	0.353	1.700 (0.666–4.123)	0.522	1.167 (0.736–1.853)
Stage IV	0.765	1.106 (0.569–2.147)	0.070	2.253 (0.607–8.369)
B symptoms	0.320	1.528 (0.652–2.321)	0.218	1.363 (0.795–2.339)
Blastoid variant	0.415	0.850 (0.528–1.859)	0.650	0.863 (0.472–1.578)
LDH increased	0.405	0.444 (0.650–2.006)	0.390	0.609 (0.450–1.890)
β2 microglobulin increased	0.601	2.021 (0.555–4.002)	0.777	2.021 (0.555–4.002)
Bulky disease	0.030	2.449 (1.093–5.503)	0.301	0.745 (0.445–1.245)
Splenomegaly	0.858	1.045 (0.640–1.706)	0.266	0.778 (0.503–1.202)
Ki-67 score high	0.014	2.079 (1.156–3.740)	0.761	1.079 (0.655–1.775)
MIPI score high	< 0.001	2.626 (1.574–4.384)	0.596	1.130 (0.712–1.793)
Metabolic response	< 0.001	5.184 (2.727–9.852)	0.917	1.028 (0.599–1.768)
SUVbw[a]	0.685	1.105 (0.681–1.792)	0.489	1.165 (0.751–1.809)
SUVlbm[a]	0.351	1.261 (0.774–2.055)	0.802	1.057 (0.685–1.631)
SUVbsa[a]	0.218	1.360 (0.833–2.221)	0.465	1.176 (0.762–1.185)
MTV[a]	< 0.001	2.344 (1.431–3.839)	0.308	0.797 (0.509–1.247)
TLG[a]	0.001	2.220 (1.348–3.655)	0.338	0.800 (0.514–1.247)
Dmax[a]	0.304	1.299 (0.788–2.143)	0.039	1.590 (1.031–2.452)
Dmax bsa[a]	0.106	1.489 (0.917–2.416)	0.037	1.587 (1.00–2.467)

Abbreviations: bsa, body surface area; bw, body weight; CI, confidence interval; HR, hazard ratio; lbm, lean body mass; MTV, total metabolic tumor volume; *N*°, number; OS, overall survival; PFS, progression free survival; SUV, standard uptake value; TLG, total lesion glycolysis.
[a]Dichotomized according to ROC analysis.

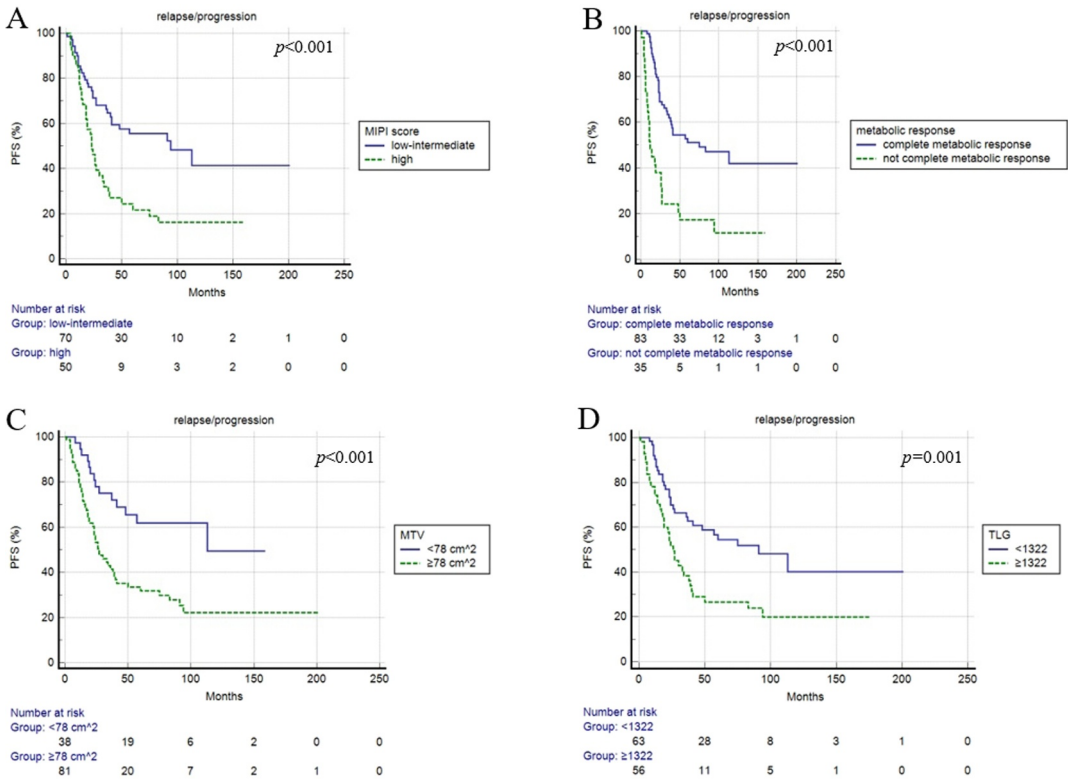

FIGURE 2 | Progression free survival curves according to MIPI score (A), metabolic response (B), MTV (C) and TLG (D).

10991069, 2025, 1, Downloaded from https://onlinelibrary.wiley.com/doi/10.1002/hon.70009 by Anna Talin - Cochraneltalia , Wiley Online Library on [29/11/2024]. See the Terms and Conditions (https://onlinelibrary.wiley.com/terms-and-conditions) on Wiley Online Library for rules of use; OA articles are governed by the applicable Creative Commons License

TABLE 4 | Multivariate analyses for progression free survival and overall survival.

	PFS		OS	
	***p* value**	**HR (95% CI)**	***p* value**	**HR (95% CI)**
Stage IV			0.818	0.905 (0.389–1.205)
Bulky disease	0.056	2.143 (0.998–4.550)		
Ki-67 score high	0.878	1.047 (0.580–1.890)		
MIPI score high	0.074	1.366 (0.970–1.924)		
Metabolic response	< 0.001	3.462 (1.887–6.349)		
MTV[a]	0.003	2.732 (1.387–5.382)		
TLG[a]	0.042	1.814 (1.019–3.229)		
Dmax[a]			0.134	1.120 (0.890–1.409)
Dmax bsa[a]			0.025	1.745 (1.070–2.844)

Abbreviations: CI, confidence interval; HR, hazard ratio; MTV, total metabolic tumor volume; OS, overall survival; PFS, progression free survival; TLG, total lesion glycolysis.
[a]Dichotomized according to ROC analysis.

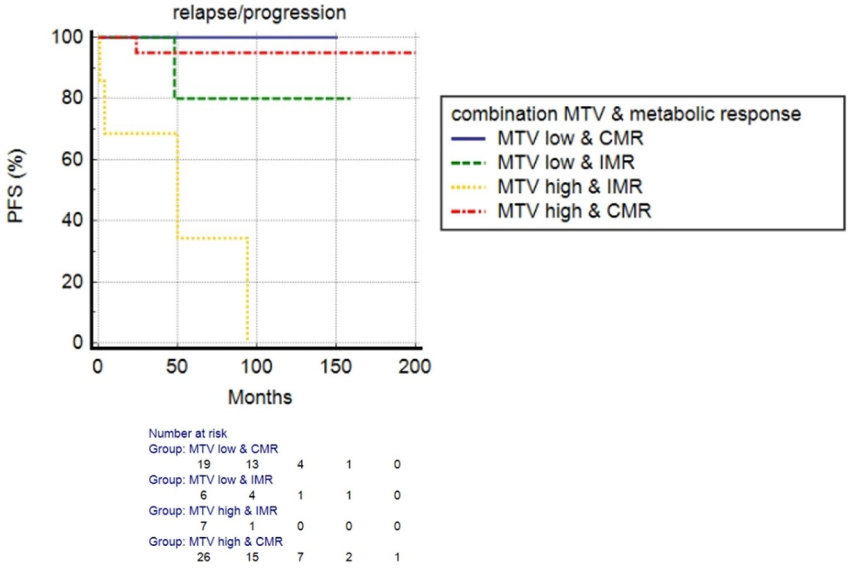

FIGURE 3 | Combination of baseline MTV and metabolic response to predict PFS.

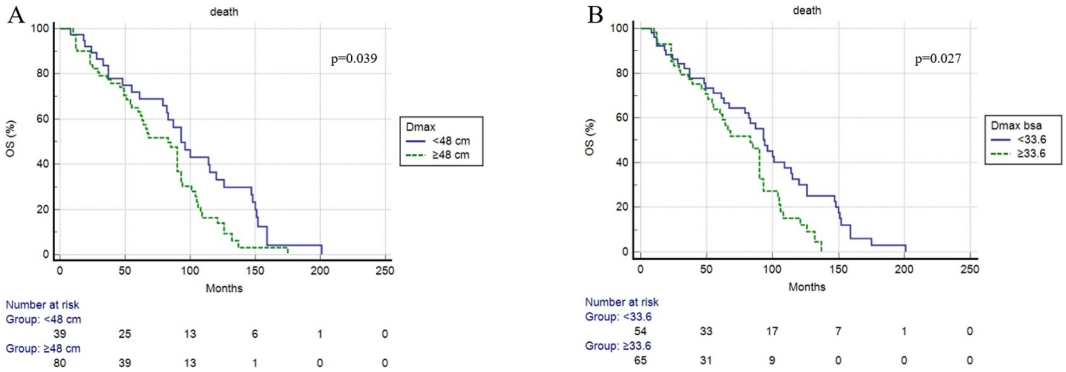

FIGURE 4 | Overall survival curves according to baseline Dmax (A) and Dmax-bsa (B).

NHL, like FL and DLBCL [11]. Also in MCL setting, this scale seems to have a strong impact [17, 18].

In our study we demonstrated that patients with a complete metabolic response after first-line therapy had significantly longer PFS than patients with incomplete response; but this finding was not confirmed for OS.

In addition to qualitative analysis, also semiquantitative baseline metabolic parameters were studied for prognostic purposes.

10991069, 2025, 1, Downloaded from https://onlinelibrary.wiley.com/doi/10.1002/hon.70009 by Anna Talin - Cochraneltalia , Wiley Online Library on [29/11/2024]. See the Terms and Conditions (https://onlinelibrary.wiley.com/terms-and-conditions) on Wiley Online Library for rules of use; OA articles are governed by the applicable Creative Commons License

Previous studies focused on the potential prognostic role of baseline SUV with controversial results [9, 19–22]. However, also in the research [20, 22] where SUVmax was demonstrated to be a good predictor of outcome the thresholds suggested were very different (i.e. 5 and 10.3). In our analysis, no SUV-related parameters (corrected for body weight, for lean body mass, for body surface area) showed to have a prognostic impact. SUV is the most widely utilized and generally accepted parameter in the current published literature because it is a feature very easy to extract, automatic and fast but less reproducible due to the potentially influence of several variables, like uptake time, decay of radiotracer, blood glucose level, risk of extravasation of tracer, lesion size and technical features (scanner-related, acquisition protocol-related and reconstruction protocol related).

To overtake these limitations, other metabolic parameters were introduced with success: MTV and TLG. These features expressed intrinsically both morphological/volumetric and metabolic characteristics of the lesions measured and demonstrated to be strong factors in several lymphoma variants [23]. Concerning MCL, positive evidence are available [9, 22] but based on low population sample. Our study confirmed the role of MTV and TLG in the largest cohort size ($n = 120$). Baseline MTV and TLG, which represent a combination of tumor volume and metabolism, were robust predictor of outcome, but only for PFS. Nevertheless, the application of MTV and TLG in clinical routine practice could probably be premature, because of the lack of a standardized method for their measurement. Different methods are proposed and a wide range of threshold levels have been used to measure the volume-based PET/CT variables. The most common method (used also in this research) utilized an isocontour threshold method based on 41% of the SUVmax, as suggested by the EANM guideline [14]. But also fixed absolute threshold (SUVmax 2.5 or SUVmax 4) or adaptive methods are described in the literature [24].

However, MTV and TLG did not consider in their definition the distribution of hypermetabolic disease and the number of lesions FDG-avid. MCL usually present with advanced stage, plural nodal localization and frequent extranodal involvement. Dmax is a parameter that represents the tumor distribution and dissemination of disease with increased uptake in the body. The potential advantages of Dmax compared to MTV and TLG are the simplicity, velocity of extraction (now automatic with different software) and clinical explanation. Moreover, Dmax is not directly affected by PET/CT tomograph characteristics or PET protocols like SUV.

However also Dmax is a variable with unexplored potential and question marks. For example, Dmax as absolute value did not consider patient body composition, like height and weight. For this reason, we decided to calculate both Dmax and Dmax corrected for body surface area applying DeBois method. This difference seemed to have an impact in our study, because in the multivariate analysis of OS only Dmax corrected for bsa showed to be an independent prognostic element.

More innovative parameters, such as sarcopenia parameters and radiomics features, are tested in the literature and also in MCL [25, 26].

Larger studies are required to find the best combination of prognostic factors and the factors most readily used in clinical practice for MCL.

Recently, Vergote et al. [10] investigated prognostic role of several PET variables (SUV, MTV, TLG and dissemination features) in untreated MCL and demonstrated that among PET features only MTV was significantly associated with PFS, while dissemination features (Dmax) had no prognostic impact. These findings were partially confirmed in our investigation, where Dmax-bsa showed to be independent prognostic factor only for OS, not for PFS.

Concerning PFS, we hypothesized a prognostic scoring system based on PET/CT metabolic features derived from the baseline and eotPET/CT scan that can be complementary and describe two different attributes of the disease: tumor burden and metabolic response after treatment. This score might possibly be helpful to predict prognosis after first-line treatment identifying patients with higher risk of recurrence/relapse. In the clinical practice, this model could anticipate the imaging controls or associate a more aggressive treatment approach after first-line. Of course, this score needs to be validated in a more robust population and with a longer follow-up period. However, the combination of both features (high baseline MTV and incomplete metabolic response) is associated with worse PFS as shown in Figure 4.

One of the main finding of this manuscript is the prognostic role of Dmax in OS, but not in PFS. The reason of this discrepancy remains unclear and deserved deeper evaluation.

The potential limitations of our study are the retrospective nature of the study, the long period of inclusion of patients, and the heterogeneity of patients (as different therapeutic regimens and clinical/epidemiological features). Despite this, so far, the present study represents the largest series of MCL investigated with a visual and semiquantitative analysis of 2-[^{18}F]FDG PET/CT and their prognostic role.

5 | Conclusion

In conclusion, with this study, we demonstrated that metabolic response at eotPET/CT (evaluated according to Deauville criteria) and the baseline metabolic tumor features (MTV and TLG) were significantly correlated with PFS. Instead, only Dmax corrected for-bsa was correlated with OS.

Acknowledgments

Open access publishing facilitated by Azienda Socio Sanitaria Territoriale degli Spedali Civili di Brescia, as part of the Wiley – SBBL agreement.

Ethics Statement

All procedures performed in studies involving human participants were in accordance with the ethical standards of the institutional and/or national research committee and with the 1964 Helsinki declaration and its later amendments or comparable ethical standards. For this type of study formal consent is not required.

10991069, 2025, 1, Downloaded from https://onlinelibrary.wiley.com/doi/10.1002/hon.70009 by Anna Talin - CochraneItalia , Wiley Online Library on [29/11/2024]. See the Terms and Conditions (https://onlinelibrary.wiley.com/terms-and-conditions) on Wiley Online Library for rules of use; OA articles are governed by the applicable Creative Commons License

Consent

Informed consent was obtained from all individual participant included in the study.

Conflicts of Interest

The authors declare no conflicts of interest.

Data Availability Statement

The data that support the findings of this study are available on request from the corresponding author. The data are not publicly available due to privacy or ethical restrictions.

Peer Review

The peer review history for this article is available at https://www.webofscience.com/api/gateway/wos/peer-review/10.1002/hon.70009.

References

1. P. Jain and M. L. Wang, "Mantle Cell Lymphoma in 2022-A Comprehensive Update on Molecular Pathogenesis, Risk Stratification, Clinical Approach, and Current and Novel Treatments," *American Journal of Hematology* 97, no. 5 (May 2022): 638–656, https://doi.org/10.1002/ajh.26523.

2. J. O. Armitage and D. L. Longo, "Mantle-Cell Lymphoma," *New England Journal of Medicine* 386, no. 26 (June 2022): 2495–2506, https://doi.org/10.1056/NEJMra2202672.

3. M. R. Wilson, A. Barrett, C. Y. Cheah, and T. A. Eyre, "How I Manage Mantle Cell Lymphoma: Indolent Versus Aggressive Disease," *British Journal of Haematology* 201, no. 2 (April 2023): 185–198, https://doi.org/10.1111/bjh.18697.

4. E. Hoster, M. Dreyling, W. Klapper, et al., "A New Prognostic Index (MIPI) for Patients With Advanced-Stage Mantle Cell Lymphoma," *Blood* 111, no. 2 (2008): 558–565, https://doi.org/10.1182/blood-2007-06-095331.

5. M. Tiemann, C. Schrader, W. Klapper, et al., "Histopathology, Cell Proliferation Indices and Clinical Outcome in 304 Patients With Mantle Cell Lymphoma (MCL): A Clinicopathological Study From the European MCL Network," *British Journal of Haematology* 131, no. 1 (2005): 29–38, https://doi.org/10.1111/j.1365-2141.2005.05716.x.

6. E. Hoster, A. Rosenwald, F. Berger, et al., "Prognostic Value of Ki-67 Index, Cytology, and Growth Pattern in Mantle-Cell Lymphoma: Results From Randomized Trials of the European Mantle Cell Lymphoma Network," *Journal of Clinical Oncology* 34, no. 12 (April 2016): 1386–1394, https://doi.org/10.1200/JCO.2015.63.8387.

7. L. Hernandez, T. Fest, M. Cazorla, et al., "p53 Gene Mutations and Protein Overexpression Are Associated With Aggressive Variants of Mantle Cell Lymphomas," *Blood* 87, no. 8 (1996): 3351–3359, https://doi.org/10.1182/blood.v87.8.3351.bloodjournal8783351.

8. D. Albano, R. Laudicella, P. Ferro, et al., and Young Italian Association of Nuclear Medicine, "The Role of 18F-FDG PET/CT in Staging and Prognostication of Mantle Cell Lymphoma: An Italian Multicentric Study," *Cancers* 11, no. 12 (November 2019): 1831, https://doi.org/10.3390/cancers11121831.

9. D. Albano, G. Bosio, N. Bianchetti, et al., "Prognostic Role of Baseline 18F-FDG PET/CT Metabolic Parameters in Mantle Cell Lymphoma," *Annals of Nuclear Medicine* 33, no. 7 (July 2019): 449–458, https://doi.org/10.1007/s12149-019-01354-9.

10. V. K. J. Vergote, G. Verhoef, A. Janssens, et al., "[18F]FDG-PET/CT Volumetric Parameters Can Predict Outcome in Untreated Mantle Cell Lymphoma," *Leukemia and Lymphoma* 64, no. 1 (January 2023): 161–170, https://doi.org/10.1080/10428194.2022.2131415.

11. B. D. Cheson, R. I. Fisher, S. F. Barrington, et al., "Recommendations for Initial Evaluation, Staging, and Response Assessment of Hodgkin and Non-hodgkin Lymphoma: The Lugano Classification," *Journal of Clinical Oncology* 32, no. 27 (2014): 3059–3068, https://doi.org/10.1200/jco.2013.54.8800.

12. D. Albano, G. Treglia, F. Dondi, et al., "18F-FDG PET/CT Maximum Tumor Dissemination (Dmax) in Lymphoma: A New Prognostic Factor?," *Cancers* 15, no. 9 (2023): 2494, https://doi.org/10.3390/cancers15092494.

13. C. Nioche, F. Orlhac, S. Boughdad, et al., "LIFEx: A Freeware for Radiomic Feature Calculation in Multimodality Imaging to Accelerate Advances in the Characterization of Tumor Heterogeneity," *Cancer Research* 78, no. 16 (2018): 4786–4789, https://doi.org/10.1158/0008-5472.can-18-0125.

14. R. Boellaard, R. Delgado-Bolton, W. J. Oyen, et al., "FDG PET/CT: EANM Procedure Guidelines for Tumour Imaging: Version 2.0," *European Journal of Nuclear Medicine and Molecular Imaging* 42, no. 2 (2015): 328–354, https://doi.org/10.1007/s00259-014-2961-x.

15. D. Dubois and E. F. Dubois, "A Formula to Estimate the Approximate Surface Area if Height and Weight Be Known," *Archives of Internal Medicine* 17 (1916): 863–871.

16. D. Albano, G. Treglia, M. Gazzilli, E. Cerudelli, R. Giubbini, and F. Bertagna, "18F-FDG PET or PET/CT in Mantle Cell Lymphoma," *Clinical Lymphoma, Myeloma & Leukemia* 20, no. 7 (July 2020): 422–430, https://doi.org/10.1016/j.clml.2020.01.018.

17. P. Klener, E. Fronkova, D. Belada, et al., "Alternating R-CHOP and R-Cytarabine Is a Safe and Effective Regimen for Transplant-Ineligible Patients With a Newly Diagnosed Mantle Cell Lymphoma," *Hematological Oncology* 36, no. 1 (2018): 110–115, https://doi.org/10.1002/hon.2483.

18. D. Lamonica, D. A. Graf, M. C. Munteanu, and M. S. Czuczman, "18F-FDG PET for Measurement of Response and Prediction of Outcome to Relapsed or Refractory Mantle Cell Lymphoma Therapy With Bendamustine-Rituximab," *Journal of Nuclear Medicine* 58, no. 1 (2017): 62–68, https://doi.org/10.2967/jnumed.116.173542.

19. P. J. Hosein, V. H. Pastorini, F. M. Paes, et al., "Utility of Positron Emission Tomography Scans in Mantle Cell Lymphoma," *American Journal of Hematology* 86, no. 10 (October 2011): 841–845, https://doi.org/10.1002/ajh.22126.

20. M. Karam, A. Ata, K. Irish, et al., "FDG Positron Emission Tomography/Computed Tomography Scan May Identify Mantle Cell Lymphoma Patients With Unusually Favorable Outcome," *Nuclear Medicine Communications* 30, no. 10 (October 2009): 770–778, https://doi.org/10.1097/MNM.0b013e32832e0c13.

21. C. Bodet-Milin, C. Touzeau, C. Leux, et al., "Prognostic Impact of 18F-Fluoro-Deoxyglucose Positron Emission Tomography in Untreated Mantle Cell Lymphoma: A Retrospective Study From the GOELAMS Group," *European Journal of Nuclear Medicine and Molecular Imaging* 37, no. 9 (August 2010): 1633–1642, https://doi.org/10.1007/s00259-010-1469-2.

22. C. Bailly, T. Carlier, A. Berriolo-Riedinger, et al., "Prognostic Value of FDG-PET in Patients With Mantle Cell Lymphoma: Results From the LyMa-PET Project," *Haematologica* 105, no. 1 (January 2020): e33–e36, https://doi.org/10.3324/haematol.2019.223016.

23. F. Tutino, E. Giovannini, S. Pastorino, O. Ferrando, G. Giovacchini, and A. Ciarmiello, "Methodological Aspects and the Prognostic Value of Metabolic Tumor Volume Assessed With 18F-FDG PET/CT in Lymphomas," *Current Radiopharmaceuticals* 15, no. 4 (2022): 259–270, https://doi.org/10.2174/1874471015666220329120631.

24. H. J. Im, T. Bradshaw, M. Solaiyappan, and S. Y. Cho, "Current Methods to Define Metabolic Tumor Volume in Positron Emission Tomography: Which One Is Better?," *Nuclear Medicine Molecular Imaging* 52, no. 1 (Febuary 2018): 5–15, https://doi.org/10.1007/s13139-017-0493-6.

25. D. Albano, N. Pasinetti, F. Dondi, R. Giubbini, A. Tucci, and F. Bertagna, "Prognostic Role of Pre-Treatment Metabolic Parameters and Sarcopenia Derived by 2-[18f]-FDG PET/CT in Elderly Mantle Cell

10991069, 2025, 1, Downloaded from https://onlinelibrary.wiley.com/doi/10.1002/hon.70009 by Anna Talin - Cochraneltalia , Wiley Online Library on [29/11/2024]. See the Terms and Conditions (https://onlinelibrary.wiley.com/terms-and-conditions) on Wiley Online Library for rules of use; OA articles are governed by the applicable Creative Commons License

Lymphoma," *Journal of Clinical Medicine* 11, no. 5 (Febuary 2022): 1210, https://doi.org/10.3390/jcm11051210.

26. M. E. Mayerhoefer, C. C. Riedl, A. Kumar, et al., "Radiomic Features of Glucose Metabolism Enable Prediction of Outcome in Mantle Cell Lymphoma," *European Journal of Nuclear Medicine and Molecular Imaging* 46, no. 13 (December 2019): 2760–2769, https://doi.org/10.1007/s00259-019-04420-6.

Supporting Information

Additional supporting information can be found online in the Supporting Information section.

10991069, 2025, 1, Downloaded from https://onlinelibrary.wiley.com/doi/10.1002/hon.70009 by Anna Talin - Cochraneltalia , Wiley Online Library on [29/11/2024]. See the Terms and Conditions (https://onlinelibrary.wiley.com/terms-and-conditions) on Wiley Online Library for rules of use; OA articles are governed by the applicable Creative Commons License

European Association of Nuclear Medicine

CERTIFICATE OF ATTENDANCE

This is to certify that

Anna Talin

Attended the

35th Annual Congress of the
European Association of Nuclear Medicine –
EANM'22 | October 15 - 19, 2022 |
Barcelona, Spain

Prof. Stefano Fanti
EANM Congress Chair 2020 – 2022

October 2022

EANM Executive Office | Schmalzhofgasse 26 | 1060 Vienna | Austria
Phone: +43 1 890 44 27 | Fax: +43 1 890 44 27-9 | office@eanm.org | www.eanm.org

European Association of Nuclear Medicine

CERTIFICATE OF ATTENDANCE

This is to certify that

Anna Talin

attended the

37th Annual Congress of the European Association of Nuclear Medicine EANM´24 | October 19–23, 2024 Hamburg, Germany

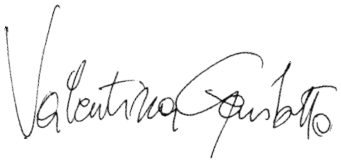

Dr. Valentina Garibotto
EANM Congress Chair 2023–2025

Hamburg, October 2024

EANM Executive Office | Schmalzhofgasse 26 | 1060 Vienna | Austria
Phone: +43 1 890 44 27 | Fax: +43 1 890 44 27-9 | office@eanm.org | www.eanm.org